Journal of Asian Earth Sciences 67–68 (2013) 138–152

Contents lists available at SciVerse ScienceDirect

Journal of Asian Earth Sciences

journal homepage: www.elsevier.com/locate/jseaes

Elemental and strontium isotopic geochemistry of the soil profiles developed on limestone and sandstone in karstic terrain on Yunnan-Guizhou Plateau, China: Implications for chemical weathering and parent materials

Wen-Jing Liu [a,c], Cong-Qiang Liu [a,b,*], Zhi-Qi Zhao [b], Zhi-Fang Xu [a], Chong-Shan Liang [b], Long-bo Li [b,c], Jia-Yi Feng [b,c]

[a] Key Laboratory of Engineering Geomechanics, Institute of Geology and Geophysics, Chinese Academy of Sciences, Beijing 100029, China
[b] State Key Laboratory of Environmental Geochemistry, Institute of Geochemistry, Chinese Academy of Sciences, Guiyang, Guizhou 550002, China
[c] University of Chinese Academy of Sciences, Beijing 100049, China

ARTICLE INFO

Article history:
Received 1 November 2012
Received in revised form 29 January 2013
Accepted 19 February 2013
Available online 27 February 2013

Keywords:
Limestone and yellow sandstone soil
Red residua
Chemical composition
Sr isotope
Chemical weathering

ABSTRACT

The limestone and yellow sandstone soil profiles from SW China were measured for chemical and Sr isotope compositions of the bulk soils and their sequential leachates (labile, carbonate, and residue or silicate fraction), aiming to characterize the parent materials of the soils, to understand the soil weathering and formation processes, and to discuss the origin of the red residua (terra rossa). The studied yellow sandstone soil, yellow limestone soil, and black limestone soil show different pH values, SiO_2 contents, Rb/Sr abundance ratios, and $^{87}Sr/^{86}Sr$ ratios. The sequential leachates of different soil types also have different $^{87}Sr/^{86}Sr$ and Ca/Sr ratios. The major chemical compositions of the studied soil profiles suggest that all the sandstone and limestone soils are developing at a stage that feldspar is exhausting and the clay minerals are changing from smectite to kaolinite and gibbsite. As compared with the red residua distributed in the karst region, the soils studied here show lower CIA values (58–84), but both higher Na_2O/K_2O (0.9–2.7) and Na_2O/Al_2O_3 concentration ratios (0.07–0.26) on average, suggesting a lower weathering intensity than that of the red residua. The depth profiles of soil CIA values, Na_2O/K_2O and Rb/Sr ratios, and $^{87}Sr/^{86}Sr$ ratios indicate that the weathering intensity is slightly lower for the upper and higher for the deeper soils, which suggest that the sandstone and limestone soil profiles were formed through both accumulation and weathering of in situ weathering residue and input of external detritus or soil from upper land. During weathering of the soils, preferential release of Ca and retention of Sr in soil result in higher Ca/Sr ratios in both labile and carbonate fractions than those in the residue fractions of all soil profiles. The co-variations of Hf/Nb and Zr/Nb ratios, together with those Rb/Sr and $^{87}Sr/^{86}Sr$ ratios of limestone soils, sandstone soils, and the red residua, demonstrate that their parent materials are distinct, and support the point that the widely distributed red residua is originated from the weathering residua of both carbonate and silicate clastic rocks, and further weathering of the weathering residua resulted in intensive release of Si, Na, Ca and relative enrichment of Al, K and other immobile elements in the red residua.

1. Introduction

Research on the identification of soil parental materials, chemical weathering of rocks and pedogenesis holds significance in the study of river basin erosion, element transportation to oceans, elemental biogeochemical cycling at the interface of rock–soil–vegetation system (Taylor and Velbel, 1991; Taylor and Lasaga, 1999; Vance et al., 2009). In addition, rock weathering processes provide inorganic nutrients in soils, buffer watershed acidification, and affect the global carbon cycle and long-term climate change (White and Brantley, 1995; Dessert et al., 2003; Clow and Mast, 2010), which relate themselves with critical societal concerns on the living environment of human beings to a deep extent. The karst area of southwest China is characterized by rare soil distributions, low soil-formation rate, along with serious water loss and soil erosion, all of which result in a fragile ecosystem (Liu, 2009). To recover and improve the deteriorating ecosystem in karst area of southwest China, a better understanding of elemental biogeochemical cycling in the interface of rock–soil–vegetation is imperative, and a systematic study on rock weathering and pedogenesis is of key importance.

* Corresponding author at: Key Laboratory of Engineering Geomechanics, Institute of Geology and Geophysics, Chinese Academy of Sciences, Beijing 100029, China. Fax: +86 851 5891609.
E-mail address: liucongqiang@vip.skleg.cn (C.-Q. Liu).

1367-9120/$ - see front matter © 2013 Elsevier Ltd. All rights reserved.
http://dx.doi.org/10.1016/j.jseaes.2013.02.017

Different from the silicate weathering, carbonate dissolution takes place over large scales at a rapid rate, but leaves small quantities of material for soil formation in karst areas. In the karst areas of southwest China, soil layers are usually thin, about 20–30 cm thick on average. The rock–soil profile in karst areas generally has a nearly clear-cut soil–rock interface, and is absent of the gradual weathering zones that are composed of weathering frontier, saprolite, and pedogenic front in most in situ rock weathering profiles (Ruxton and Berry, 1957; Sequeira Braga et al., 2002; Kirschbaum et al., 2005; Ma et al., 2007). Yellow soil (developed on both sandstone and limestone) and limestone soil (developed from limestone weathering) are the two main types of soil in this area, and their source materials and formation processes still remain controversial. In particular, the origin of the thick and widely distributed yellow or reddish-yellow soil layer or mantle developed on carbonate rocks, also called red residua or terra rossa (Ji et al., 2004; Feng et al., 2009b), has been attracting wide and intense interests from both geochemists and pedologists for many years.

The red residua is a type of red clay soil produced by the weathering of limestone (Durn et al., 1999). When limestone weathers, the clay contained in the rocks is left behind, along with any other non-soluble rock material. Under oxidizing conditions, when the soils are above the water table, iron oxide (rust) forms in the clay. This gives it a characteristic red to orange color. However, the origin of the red residua is still on the debate about their parent material sources. As reviewed by Feng et al. (2009b), there are at least six theories describing the origin of the worldwide distributed reddish-yellow soil at present, which are *the residual theory* (Moresi and Mongelli, 1988; Ji et al., 2004), *the allochthonous theory* (Hall, 1976; Olson et al., 1980; Prasad, 1983), *the non-carbonate rock weathering theory* (Driese et al., 2003; Cooke et al., 2007), *the eolian theory* (Syers et al., 1969; Macleod, 1980; Mee et al., 2004), *the iso-volumetric weathering theory* (Stephenson, 1939; Monroe, 1986; Li and Wang, 1988; Merino and Banerjee, 2008), and *the poly-origin theory* (Yaalon and Ganor, 1973; Jackson, 1982; Durn et al., 1999). In all of the theories, the principal debate regards the source material of the soil.

The studies carried out recently on the origin of the red residua on the Yunnan-Guizhou Plateau support the residual theory, suggesting that the red residua with underlying carbonate rocks is in situ weathering solum, and originates mostly from insoluble residues of the parent carbonate rocks (Wang et al., 1999; Ji et al., 2004; Feng and Zhu, 2009; Feng et al., 2009a). Their arguments for the residual origin stems mostly from the studies of quartz content, size distribution of quartz grains, mineral composition, surface micro-texture and crystal morphology of quartz, oxygen isotope ratios of quartz, and other tracers. Nevertheless, the red residua (terra rossa) is unlikely to have been formed from in situ weathering of carbonate rocks due to mass budget problem, because the carbonate rocks generally contain a small amount (on average, at most 5% in mass fraction of carbonate rocks) of insoluble silicate materials. Moreover, the geochemical evidence supporting the origin of the in situ weathering of carbonate rocks is still insufficient, and more evidence such as the major and trace element, Sr and other isotope evidence is needed. In particular, more systematic comparison studies on the geochemical features of different soil profiles developed on clastic rocks such as sandstone, shale, and carbonate rocks are necessary to document the origin relationship between the vastly distributed yellow soil, limestone soil, and the red residua in karst area.

Major and trace elements, as well as Sr isotopes are powerful tools in the studies of rock weathering and pedogenesis, especially when applied to source material identification, characterization of soil formation pattern, and rock weathering degree (Worden and Compston, 1973; Kronberg et al., 1987; Maynard, 1992; Nesbitt et al., 1996; Malpas et al., 2001; Stewart et al., 2001; Ma et al., 2007, 2010). This study first focuses on the major and trace element, and Sr isotope geochemistry of the yellow sandstone soil as well as both black and yellow limestone soil profiles in central Guizhou province, southwest China. A three-step sequence extraction procedure was also carried out on the soil samples. Ca and Sr contents, along with $^{87}Sr/^{86}Sr$ ratio were determined for different phases to provide further information of chemical weathering and soil formation processes. Combined with a large number of previous work published on red residua in this area (Sun et al., 2002; Wang et al., 2002, 2007; Ji et al., 2004; Liu et al., 2004), the results obtained here may provide insight into the origin of the red residua, in addition to the weathering and pedogenesis of sandstone and limestone in the karst area on Yunnan-Guizhou Plateau, China.

2. Regional lithology and geography

Guizhou Province is located in the west of the Yangtze Platform. The Yangtze Platform spread from the east of Sichuan province, alone Changjiang river, and to the east part of south China. It was in a marine environment from Sinian to the middle of Triassic and received a thickness of more than ten thousand meters of continuous sedimentary rocks. In Guizou Province, the carbonate deposition reached a total thickness of approximately 8500 m. More than 70% of the outcropped rocks there are carbonate rocks (both limestone and dolomite) and the rest are mainly clastic rocks, with piecemeal igneous and epi-metamorphic rocks. The strata distributed in Guizhou Province, together with in eastern Yunnan, southern Sichuan and western Guangxi Province are of Precambrian and Triassic ages for carbonate rocks and of Permian age for arenaceous shale. The carbonate rocks are commonly interbedded with clastic rocks (Fig. 1). The widely distributed carbonate rocks in southwest China form one of the largest continuous distributions of karst landform in the world, with an area of about 500,000 km^2 (Young and Nesbitt, 1998).

As a main part of the Yunnan-Guihzou Plateau, Guizhou Province has a mean annual temperature of 8–12 °C and a mean annual rainfall of 850–1600 mm. More than 50% of the rainfall occurs during June and August. Guizhou is located in the transition zone of the second and third tread of Chinese hypsography, with an average altitude of about 1100 m, displaying a topography slopping from west to the east within the province. Carbonate mesa, peak cluster and forest, basins and hills dominate the types of landforms in Guizhou.

The yellow and limestone soil are the major soil types in this region, occupying 46.5% and 17.6% of total soil area of Guizhou province (Liu and Zhang, 1997). Additionally, red residua, generally with a thickness of 8–10 m, extensively developed in karst area. The distribution of the red residua is controlled mainly by karst geomorphological, hydrological, and ecological environments (Zhu and Li, 2004).

3. Soil profiles and analytical methods

3.1. Soil profiles

To study the rock chemical weathering processes occurring in karstic areas and the formation of soils on sandstone and limestone rocks, three soil profiles developed on limestone and two soil profiles on sandstone were chosen. Since the carbonate rocks (both limestone and dolomite) and sandstone rocks are the main rocks in karst areas, the geochemical features of the soil profiles developed on these two types of rocks will provide important insights into the origin of the widely distributed red residua.

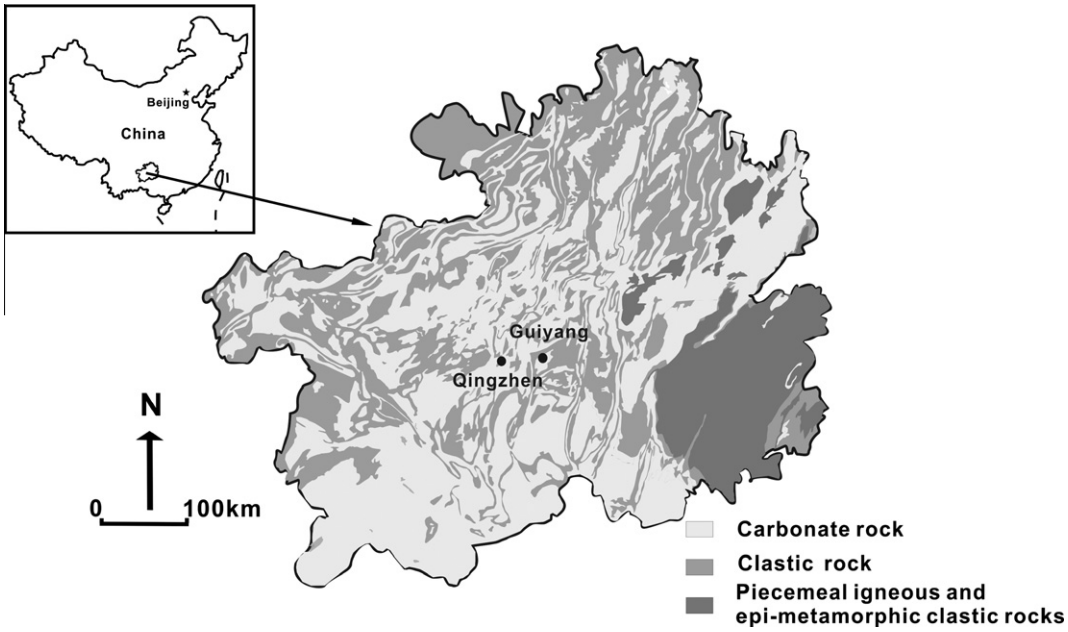

Fig. 1. Map of simplified geology of the Guizhou Province and the sampling locations.

The soil profiles were sampled in May 2009 from two areas, Baiyi, Wudang district near Guiyang city and Wangjiazhai near Qingzhen city (Fig. 1). Both sampling areas are in central Guizhou, and the soil profiles in the same area are located not far from each other, about several kilometers apart. Five soil profiles were sampled, which are BY-I and BY-II in Baiyi, and QZ-I, QZ-II and QZ-III in Wangjiazhai in the suburb of Qingzhen city. The basic information of the five soil profiles studied is listed in Table 1. A pit was dug first and then the soil samples were collected from bottom to the top of the profile, every sample representing 5 cm of span through the profile. The depth of the black limestone soil pit was limited by the clearly soil–rock interface (the typical feature of this kind of soil), and the yellow limestone soil and yellow sandstone soil profiles were dug to the layer of refusal. A Permian arenaceous shale weathering frontier sample was drilled under the yellow sandstone soil profile in Baiyi, and a Triassic limestone sample was collected under the limestone profile of QZ-I.

3.2. Analytical methods

Values of pH were determined on 1:2.5 of soil to CO_2-free pure water mixtures with a Sension 156 multiple-parameters analyzer from HACH. The major elements were analyzed by classical wet-chemical analyzing methods: Si by gravimetric-analysis; Al and Fe by volumetric-methods; Ca, Mg, K, and Na by AAS. All the errors for major element contents were less than 5%. The bulk sample were treated with 1 mol/L hydrochloric to remove the non-silicate Ca, and the residue was then digested in a mixture of nitric and hydrofluoric acid, and Ca content was determined by ICP-OES to calculate the silicate Ca content and CIA (chemical index of alteration) (Table 1). CIA was first given by Nesbitt and Young (1982) to evaluate weathering extent quantitatively in sedimentary rocks (and also articles cited there about the weathering profiles developed from basalt and granite). It is defined as $Al_2O_3/(Al_2O_3 + CaO^* + Na_2O + K_2O) * 100$ (molar contents, with CaO^* being CaO content in silicate fraction of the sample).

Bulk samples were digested with mixture of nitric and hydrofluoric acid (twice distilled purification) in the high-pressure Teflon bombs at a temperature of 190 °C for at least 48 h. As for the upper part samples of the profile, some of them are treated with drips of HNO_3–H_2O_2 to remove the organic materials. The digested samples were prepared into different medium for trace element and $^{87}Sr/^{86}Sr$ ratio measurements. The trace elements were analyzed by an ELAN DRC-e Q-ICP-MS from Perkin Elmer Company, with Rh as internal standard. The repeated analyses of AMH-1 (andesite), GBPG (garnet-biotite plagiogneiss) and OU-6 (slate) standards were processed as exterior standard to test the accuracy and precision of the method, which were within ±10%. The prepared solution was eluted through quartz cation exchange columns using AG-50W-X8 200–400 mesh resin to separate Sr from other cations. The pure Sr fraction was treated with 4% nitric acid,

Table 1
Basic features of the soil profiles studied.

Profile NO.	Sampling area	Type of soil	Longitude	Latitude	Altitude (m)	Profile depth (cm)	Type of bedrock	Landform
BY-I	Baiyi in Wudang district	Yellow sandstone soil profile	107°01′	26°47′	1214	70	Permian arenaceous shale	Hilly area
BY-II	Baiyi in Wudang district	Yellow limestone soil profile	107°00′	26°48′	1327	75	Precambrian carbonate rocks	Low-laying areas
QZ-I	Wangjiazhai in Qingzhen city	Black limestone soil profile	106°20′	26°31′	1285	65	Triassic carbonate rocks	Hilly area, in the crevice of carbonate rock
QZ-II	Wangjiazhai in Qingzhen city	Black limestone soil profile	106°20′	26°31′	1291	110	Triassic carbonate rocks	Hilly area, in the crevice of carbonate rock
QZ-III	Wangjiazhai in Qingzhen city	Yellow sandstone soil profile	106°23′	26°31′	1279	70	Permian arenaceous shale	Low-laying areas

and analyzed for $^{87}Sr/^{86}Sr$ on Nu Plasma MC-ICP-MS. Analyses of NBS-987 yielded a mean $^{87}Sr/^{86}Sr$ ratio of 0.710234 ± 0.000027 (2σ, n = 45) during the period of analysis.

Sequential extraction steps were carried out for the selected samples with an interval of 10 cm in BY-I, BY-II, QZ-I, QZ-III profiles. First, 0.5 mol/L ammonium acetate leaching (pH = 7.0) was applied to the samples (200 mesh) to remove the labile ions adsorbed to the mineral surface; second, 0.5 mol/L hydrochloric acid was added to dissolve the carbonate fraction of the soil samples; finally, nitric and hydrofluoric mixing acid was used to digest of the silicate residue. The leachates produced from the above steps were filtered through 0.45 μm cellulose acetate filters. The filtered solution was measured for Ca contents on ICP-OES and for Sr contents on ICP-MS. Before measurement of Sr isotopic composition, the Sr was separated from other solutes in the leachate and digested solution by using the same methods as the bulk sample analysis. The $^{87}Sr/^{86}Sr$ ratio was measured on TIMS (IsoProbe-T), with the $^{86}Sr/^{88}Sr$ ratio normalized to 0.1194. Analyses of NBS-987 yielded a mean $^{87}Sr/^{86}Sr$ ratio of 0.710235 ± 0.000014 (±2σ, n = 26) during the period of analysis. Since the Sr isotopic compositions of the bulk samples were measured on Nu Plasma MC-ICP-MS and those of the sequential extraction products on TIMS, the comparative measurements of Sr isotopic composition for six samples were conducted separately on the TIMS and the MC-ICP-MS. The results are comparable, with differences in $^{87}Sr/^{86}Sr$ ratio within 2 sigma errors of individual sample on the TIMS or on the MC-ICP-MS.

4. Results

4.1. Chemical compositions of the bulk soil samples

The major and trace element concentrations, pH, CIA, and $^{87}Sr/^{86}Sr$ ratios of bulk samples are listed in Table 2. The pH values vary within a range of 4.03–4.8 for yellow sandstone soil (BY-I and QZ-III), 4.82–5.6 for yellow limestone soil (BY-II), and 5.72–6.96 for black limestone soil (QZ-I and QZ-II). As for CIA, the yellow sandstone soil shows a slightly low range in general than the limestone soils. SiO_2 contents are higher in the yellow sandstone soil profiles, changing between 64.3% and 86.2%, while in limestone soils between 45.9% and 83.9%. Al_2O_3 contents are lower of the sandstone soils (Al_2O_3 = 2.43–11.2%), as compared with those of the limestone soils (Al_2O_3 = 5.2–21.2%). Yellow limestone soil is lower than black limestone soil in Al_2O_3, but higher in SiO_2 content. The lowest K_2O content is found in the sandstone soil (0.29%) while the highest in the limestone soil (1.31%), with higher average value in the limestone soils.

Table 2 also presents contents of the trace elements Zr, Hf, Nb, Rb, and Sr. The soil samples have Zr contents of 221–600 μg/g, Hf contents of 5.81–13.8 μg/g, which are not significantly different between different soil profiles. The Nb contents are the highest (55.8–62.6 μg/g) in the yellow sandstone soils (soil profile QZ-III) and the lowest (16.6–20.2 μg/g) in the yellow limestone soils (soil profile BY-II). The Rb contents are much lower in yellow sandstone soils (17.3–57.8 μg/g) as compared to black limestone soils (118.3–163 μg/g). The Sr contents are higher in sandstone soils (54.4–95.2 μg/g) than in limestone soils (36.7–60.0 μg/g).

4.2. Sr isotopic composition of bulk soil samples

The Rb/Sr and $^{87}Sr/^{86}Sr$ ratios of bulk samples from the sandstone and limestone soil profiles hold distinct values between different soil types, but both ratios increase with increasing depth in all soil types (Table 2, Fig. 2). The Rb/Sr ratios of yellow sandstone soils vary from 0.30 to 1.02 (concentration ratio); those of the yellow limestone soils from 1.14 and 1.75; those of the black limestone soils are higher, varying in the range of 2.03–3.60. As for the $^{87}Sr/^{86}Sr$ ratio, the yellow sandstone soils (BY-I and QZ-III) exhibit a lower range of 0.71049–0.71518 and the limestone soils (BY-II, QZ-I, QZ-II) show a higher range of 0.71748–0.72266.

4.3. $^{87}Sr/^{86}Sr$ and Ca/Sr ratios in different sequential leachates

Ca and Sr content, Ca/Sr and $^{87}Sr/^{86}Sr$ ratio of sequential leaching fractions of two yellow sandstone soil profiles (BY-I and QZ-III), a yellow limestone soil profile (BY-II) and a black limestone profile (QZ-I) are given in Table 3. In the limestone soil samples, the labile and carbonate fractions exhibit constant $^{87}Sr/^{86}Sr$ ratios in the same soil profile, which are within a range of 0.70832–0.70964 and significantly lower than those of the residual fraction ($^{87}Sr/^{86}Sr$ = 0.71946–0.72432). The $^{87}Sr/^{86}Sr$ ratios of the residual phase are nearly constant with those of the bulk samples, and increase with increasing depth in the soil profiles (Fig. 3). In contrast to the limestone soils, the yellow sandstone soils show significantly variable $^{87}Sr/^{86}Sr$ ratios of both labile and residual fractions. The labile and carbonate fractions from the sandstone soil profile BY-I exhibit a wide variation of $^{87}Sr/^{86}Sr$ ratios of 0.70946–0.71271, while those from the sandstone soil profile QZ-III have $^{87}Sr/^{86}Sr$ ratios varying between 0.70945 and 0.71226. The residual fraction of the sandstone soil profile BY-I show $^{87}Sr/^{86}Sr$ ratios of 0.71022–0.71450, while that of the sandstone soil profile QZ-III shows a narrow range (0.71078–0.71135) of $^{87}Sr/^{86}Sr$ ratios. The depth profiles of $^{87}Sr/^{86}Sr$ ratios of labile and carbonate fractions in the soil profile BY-I show higher values at the upper depth and the lowest values at the bottom. In the upper part of the soil profile, the $^{87}Sr/^{86}Sr$ ratios of the labile and carbonate fractions are higher than those of the residual material and bulk soil sample. For the soil profile QZ-III, the $^{87}Sr/^{86}Sr$ ratios of all the fractions are similar, which show a slightly increasing trend from top to the bottom of the soil profile. The Ca/Sr ratios of residual fractions are significantly lower than those of the labile and carbonate fractions in all of the soil profiles (Fig. 4), of which the residual fraction of the yellow sandstone soils show lower Ca/Sr ratios compared to those of the limestone soils. The yellow limestone and black limestone soils have Ca/Sr ratios of 69–100 and 36–53 in the residual fractions, respectively. The yellow limestone soil show a range of Ca/Sr ratios between 399 and 870 for labile and carbonate fraction, while the corresponding range for the labile and carbonate fractions of black limestone soil is 288–688. The labile and carbonate fractions of the yellow sandstone soil profiles (BY-I and QZ-III) are in the range of 512–3088, significantly higher than those of the limestone soils. Though variable, the Ca/Sr ratios of the labile and carbonate fractions of the yellow limestone soil profile generally increase with increasing soil depth (Fig. 4a). The depth profile of the Ca/Sr ratios in both labile and carbonate fractions of other soil profiles (Fig. 4b–d) are generally independent of soil depth.

5. Discussion

5.1. Chemical weathering of the soils

5.1.1. Comparison of elemental geochemical proxies of the bulk samples

A-CN-K and A-CNK-FM ternary diagrams portray the molar proportions of Al_2O_3 (A apex), $CaO^* + Na_2O$ (CN apex), K_2O (K apex), and $FeO_T + MgO$ (FM apex) for the bulk samples (Fig. 5), which are widely used to discuss the weathering extent and trend prediction of in situ weathering profiles (Nesbitt and Young, 1984, 1989). As illustrated in Fig. 5, all the sandstone and limestone soil profiles are developing at a stage that feldspar is exhausting and the clay

Table 2
Major and trace element contents and $^{87}Sr/^{86}Sr$ ratios of bulk samples of soil profiles studied and potential sources.

Sample (depth cm)	pH	Ca * O (%)	CIA	SiO_2 (%)	Al_2O_3 (%)	$Fe_2O_3^T$ (%)	CaO (%)	MgO (%)	K_2O (%)	Na_2O (%)	Zr (μg/g)	Hf (μg/g)	Nb (μg/g)	Rb (μg/g)	Sr (μg/g)	Rb/Sr	$^{87}Sr/^{86}Sr$
BY-I (0–5)	4.22	0.03	80.5	75.6	5.00	4.41	0.22	0.46	0.29	0.51	238	5.81	33.6	19.3	56.7	0.34	0.71072
BY-I (5–10)	4.20	0.03	79.1	82.2	4.52	3.67	0.18	0.45	0.3	0.49	259	6.01	34.0	18.4	56.8	0.32	0.71063
BY-I (10–15)	4.22	0.04	74.3	84.4	3.54	3.77	0.18	0.47	0.32	0.49	261	6.28	34.2	17.8	54.4	0.33	0.71063
BY-I (15–20)	4.08	0.04	63.1	86.2	2.43	3.83	0.16	0.46	0.29	0.63	259	6.50	34.8	17.3	56.0	0.31	0.71056
BY-I (20–25)	4.08	0.04	67.7	85.2	3.47	3.65	0.17	0.41	0.29	0.77	258	6.37	35.8	17.4	57.2	0.30	0.71049
BY-I (25–30)	4.03	0.04	69.3	85.2	3.39	3.60	0.21	0.47	0.29	0.68	260	6.29	35.1	17.4	56.4	0.31	0.71050
BY-I (30–35)	4.12	0.04	78.5	85.5	4.32	3.07	0.15	0.43	0.28	0.49	236	6.23	32.9	17.8	58.6	0.30	0.71063
BY-I (35–40)	4.19	0.03	79.4	84.4	5.30	3.25	0.19	0.46	0.34	0.58	269	7.63	39.0	23.6	61.6	0.38	0.71104
BY-I (40–45)	4.42	0.04	77.7	80.5	7.10	3.72	0.18	0.62	0.45	0.90	280	6.73	36.8	28.7	57.7	0.50	0.71167
BY-I (45–50)	4.32	0.02	84.4	77.7	8.15	4.76	0.18	0.7	0.49	0.57	292	6.97	39.3	30.4	58.5	0.52	0.71171
BY-I (50–55)	4.80	0.03	68.9	72.6	8.31	5.88	0.31	1.07	0.8	1.71	295	8.25	41.8	44.5	57.3	0.78	0.71274
BY-I (55–60)	4.49	0.03	71.5	72.9	8.60	5.71	0.44	1.04	0.76	1.55	319	7.62	44.0	34.9	66.1	0.53	0.71202
BY-I (60–65)	4.64	0.03	80.5	70.9	10.7	5.83	0.21	0.96	0.79	1.03	319	7.48	38.7	45.6	56.7	0.80	0.71372
BY-I (65–70)	4.57	0.04	79.4	68.1	11.2	6.89	0.17	1.06	0.95	1.09	340	8.42	40.1	56.2	54.9	1.02	0.71518
BY-II (0–5)	4.82	0.12	67.7	77.4	5.22	2.98	0.35	0.56	0.47	1.07	232	6.36	16.9	48.5	36.8	1.32	0.71748
BY-II (5–10)	4.99	0.11	72.5	80.0	5.74	2.77	0.25	0.6	0.58	0.82	265	6.27	16.6	49.9	43.8	1.14	0.71808
BY-II (10–15)	5.20	0.12	77.2	82.0	6.20	3.13	0.29	0.64	0.5	0.65	259	7.10	18.5	52.9	39.2	1.35	0.71951
BY-II (15–20)	5.33	0.12	74.3	83.9	5.16	3.05	0.49	0.66	0.52	0.61	266	7.41	18.6	57.2	37.9	1.51	0.71925
BY-II (20–25)	5.39	0.11	73.9	82.6	6.00	3.14	0.56	0.67	0.45	0.87	272	7.55	18.8	59.9	38.3	1.56	0.71940
BY-II (25–30)	5.42	0.11	76.1	82.0	6.22	2.88	0.6	0.68	0.56	0.7	283	7.79	19.2	60.3	38.6	1.56	0.71934
BY-II (30–35)	5.45	0.13	75.8	82.3	5.70	3.22	0.89	0.67	0.52	0.62	270	7.51	18.8	62.7	38.2	1.64	0.71946
BY-II (35–40)	5.48	0.12	78.6	80.6	6.92	3.56	0.88	0.7	0.54	0.66	257	7.23	19.8	63.2	38.4	1.65	0.71929
BY-II (40–45)	5.49	0.10	80.7	79.7	7.15	3.44	0.96	0.69	0.59	0.54	249	7.10	19.0	64.0	36.7	1.75	0.71949
BY-II (45–50)	5.51	0.10	75.2	79.2	7.02	3.63	1.16	0.73	0.67	0.86	256	7.20	19.5	67.5	38.7	1.74	0.71962
BY-II (50–55)	5.53	0.11	83.7	77.7	9.26	3.57	0.70	0.70	0.60	0.58	253	7.10	19.4	66.6	39.1	1.71	0.71954
BY-II (55–60)	5.55	0.10	84.2	77.1	10.3	3.54	0.26	0.74	0.59	0.67	242	6.90	19.4	66.3	38.6	1.72	0.71970
BY-II (60–65)	5.53	0.10	80.4	75.7	10.5	3.99	0.29	0.77	0.60	1.04	246	7.00	19.8	66.4	39.3	1.69	0.71923
BY-II (65–70)	5.53	0.10	82.5	76.7	10.0	3.64	0.39	0.73	0.63	0.76	257	7.50	20.2	68.9	41.2	1.68	0.71976
BY-II (70–75)	5.60	0.11	72.2	74.9	9.28	4.14	0.49	0.82	0.65	1.62	221	6.00	18.7	61.8	41.7	1.48	0.71928
QZ-I (0–5)	6.35	0.04	74.0	49.0	13.5	5.19	1.48	1.60	1.32	1.98	466	10.8	29.5	121	59.6	2.03	0.71812
QZ-I (5–10)	6.43	0.05	77.4	52.0	14.4	5.30	1.07	1.79	0.99	1.85	496	11.6	32.9	128	60.0	2.13	0.71834
QZ-I (10–15)	6.52	0.10	75.9	52.9	14.1	5.09	1.11	1.85	1.08	1.89	187	5.20	29.5	124	54.8	2.26	0.71897
QZ-I (15–20)	6.57	0.02	83.6	53.5	15.5	5.59	1.00	1.73	0.91	1.23	537	12.3	34.3	133	57.5	2.31	0.71933
QZ-I (20–25)	6.54	0.04	79.4	55.2	14.9	5.54	0.97	1.80	0.95	1.67	509	11.5	33.0	123	53.3	2.31	0.71923
QZ-I (25–30)	6.59	0.04	82.1	55.2	16.4	5.39	0.70	1.74	0.90	1.54	448	12.4	32.6	129	48.5	2.66	0.71961
QZ-I (30–35)	6.67	0.04	87.4	57.2	19.8	5.70	0.56	1.64	1.07	0.98	538	12.7	35.7	125	54.9	2.28	0.71965
QZ-I (35–40)	6.61	0.02	81.1	57.9	16.2	5.51	0.78	1.79	0.91	1.68	600	13.8	37.0	123	56.7	2.17	0.71975
QZ-I (40–45)	6.61	0.04	79.5	58.3	15.8	6.11	0.70	1.69	0.96	1.79	561	13.4	35.8	119	48.7	2.44	0.71966
QZ-I (45–50)	6.70		83.6	55.5	18.4	6.08	0.64	1.73	1.04	1.45	508	12.0	32.9	122	48.8	2.5	0.72026
QZ-I (50–55)	6.71	0.02	84.7	52.1	19.7	7.58	0.38	1.82	1.13	1.40	425	10.2	30.0	129	47.1	2.74	0.72096
QZ-I (55–60)	6.96	0.02	83.5	48.8	21.2	7.53	0.46	2.03	1.25	1.71	373	9.20	28.2	143	43.6	3.28	0.72224
QZ-I (60–65)	6.66	0.02	81.0	47.4	20.6	8.50	0.40	2.13	1.21	2.12	340	8.30	24.8	146	40.6	3.60	0.72266
QZ-II (0–5)	5.72	0.16	81.1	45.9	18.1	7.45	0.67	1.88	1.00	1.72	369	9.00	25.1	135	54.4	2.48	0.71847
QZ-II (5–10)	6.19	0.10	81.9	49.4	16.0	7.52	0.73	1.47	0.79	1.52	382	11.2	27.1	130	51.9	2.50	0.71865
QZ-II (10–15)	5.78	0.11	82.4	50.5	16.2	6.76	0.65	1.38	0.78	1.45	373	10.6	26.6	118	49.9	2.37	0.71842
QZ-II (15–20)	5.86	0.11	84.3	51.2	16.8	7.12	0.62	1.39	0.76	1.28	404	11.5	28.5	120	49.1	2.43	0.71898
QZ-II (20–25)	6.00	0.13	82.6	49.6	17.9	7.20	0.73	1.51	0.91	1.55	397	11.2	29.6	126.6	51.3	2.47	0.71937
QZ-II (25–30)	5.92	0.18	79.5	52.2	16.7	7.34	0.62	1.57	0.92	1.82	367	10.6	28.2	131.0	49.9	2.63	0.71952
QZ-II (30–35)	6.09	0.13	85.5	52.6	17.0	7.98	0.57	1.59	0.79	1.10	386	9.70	29.3	139	48.5	2.87	0.71957
QZ-II (35–40)	6.12	0.16	79.0	52.4	16.8	8.72	0.63	1.66	0.88	1.94	368	9.05	28.6	148	49.1	3.01	0.72043
QZ-II (40–45)	6.10	0.12	80.5	51.7	17.2	8.52	0.69	1.68	0.90	1.80	358	9.18	24.2	144	48.8	2.95	0.72030
QZ-II (45–50)	6.11	0.19	79.8	50.4	18.1	8.96	0.50	1.80	1.19	1.80	346	8.72	27.2	157	49.0	3.20	0.72137
QZ-II (50–55)	6.40	0.10	77.7	49.8	17.6	8.83	0.73	1.77	1.02	2.28	322	8.09	25.8	153	47.4	3.23	0.72089
QZ-II (55–60)	5.87	0.14	75.5	50.5	17.4	9.11	0.77	1.84	1.14	2.52	298	7.82	22.6	157	48.8	3.22	0.72110
QZ-II (60–70)	6.25	0.17	78.6	50.2	19.1	8.77	0.73	1.93	1.05	2.28	318	9.19	26.8	138.7	48.2	2.88	0.72085
QZ-II (70–80)	6.25	0.16	78.9	49.8	19.7	9.04	0.63	1.83	1.30	2.17	332	8.52	24.4	148	45.4	3.26	0.72112
QZ-II (80–90)	6.22	/	/	51.4	19.1	8.67	0.49	1.69	1.17	2.00	309	7.80	25.9	157	47.8	3.28	0.72131
QZ-II (90–100)	6.21	0.12	79.7	51.3	18.0	8.74	0.63	1.82	1.21	2.61	352	8.94	25.7	158	53.6	2.95	0.72130
QZ-II (100–110)	5.99	0.17	75.6	51.5	17.2	8.96	0.70	1.85	1.26	2.81	314	7.97	27.4	163	49.5	3.29	0.72135
QZ-III (0–5)	4.11	0.14	77.7	65.7	10.5	8.20	0.22	0.90	0.78	1.15	412	11.4	62.6	54.4	80.4	0.68	0.71167
QZ-III (5–10)	4.11	0.11	76.0	64.3	10.2	8.10	0.26	0.91	0.75	1.35	423	9.49	61.1	48.1	79.1	0.61	0.71116
QZ-III (10–15)	4.11	0.08	74.1	66.4	9.10	8.34	0.45	0.93	0.73	1.37	404	9.07	57.2	47.5	77.0	0.62	0.71099
QZ-III (15–20)	4.07	0.15	73.7	70.3	8.59	7.56	0.29	0.79	0.64	1.28	352	8.86	59.7	44.8	83.0	0.54	0.71087
QZ-III (20–25)	4.10	0.11	73.5	70.4	8.20	8.03	0.13	0.81	0.68	1.23	363	10.6	58.6	48.6	92.8	0.52	0.71078
QZ-III (25–30)	4.13	0.01	69.8	69.9	7.82	8.31	0.42	0.88	0.72	1.57	359	10.7	57.2	49.8	92.4	0.54	0.71091
QZ-III (30–35)	4.16	0.11	74.4	69.5	9.12	8.05	0.50	0.87	0.73	1.30	330	10.6	56.1	50.6	89.7	0.56	0.71091
QZ-III (35–40)	4.17	0.08	58.9	69.5	7.34	8.51	0.76	0.88	0.90	2.43	402	9.71	59.2	47.3	88.0	0.54	0.71099
QZ-III (40–45)	4.19	0.10	74.8	68.1	9.70	8.44	0.22	0.90	0.79	1.35	369	11.2	57.8	56.1	95.2	0.59	0.71122
QZ-III (45–50)	4.16	0.08	74.5	68.0	10.1	8.56	0.22	0.92	0.78	1.49	350	10.5	55.8	53.1	87.9	0.60	0.71148
QZ-III (50–55)	4.18	0.08	71.5	69.0	9.28	8.07	0.23	0.91	0.74	1.67	368	10.7	58	54.2	90.3	0.60	0.71136
QZ-III (55–60)	4.16	0.18	70.7	69.2	8.71	8.49	0.24	0.91	0.80	1.58	377	11.1	59.0	55.9	91.0	0.61	0.71129

Table 2 (*continued*)

Sample (depth cm)	pH	Ca * O (%)	CIA	SiO_2 (%)	Al_2O_3 (%)	$Fe_2O_3^T$ (%)	CaO (%)	MgO (%)	K_2O (%)	Na_2O (%)	Zr (μg/g)	Hf (μg/g)	Nb (μg/g)	Rb (μg/g)	Sr (μg/g)	Rb/Sr	$^{87}Sr/^{86}Sr$
QZ-III (60–65)	4.17	0.08	68.2	69.3	8.25	8.30	0.26	0.95	0.78	1.74	418	10.4	58.8	52.9	80.3	0.66	0.71172
QZ-III (65–70)	4.12	0.04	71.0	68.1	10.3	8.04	0.45	0.86	0.87	1.93	372	10.7	58.1	57.8	87.8	0.66	0.71173
Permian arenaceous shale weathering frontier	/	0.02	79.3	77.0	6.12	7.3	0.37	0.96	0.81	0.41	198	5.60	28.8	21.1	57.1	0.37	0.70943
Al-QZ		0.36		33.6	18.2	25.8	0.36	2.02	5.05	0.18	286	6.10	25.5	150	21.1	7.11	0.78044
Triassic limestone	/	/	/	0.78	0.1	0.25	55.2	0.30	0.13	0.20	1.00	0.10	0.04	0.10	232	/	0.70775

Note: Ca * O represents the Ca bearing in silicate fraction; Rb/Sr is in weight content ratio; AI-QZ is the acid-insoluble materials of Triassic limestone underlying QZ-I profile.

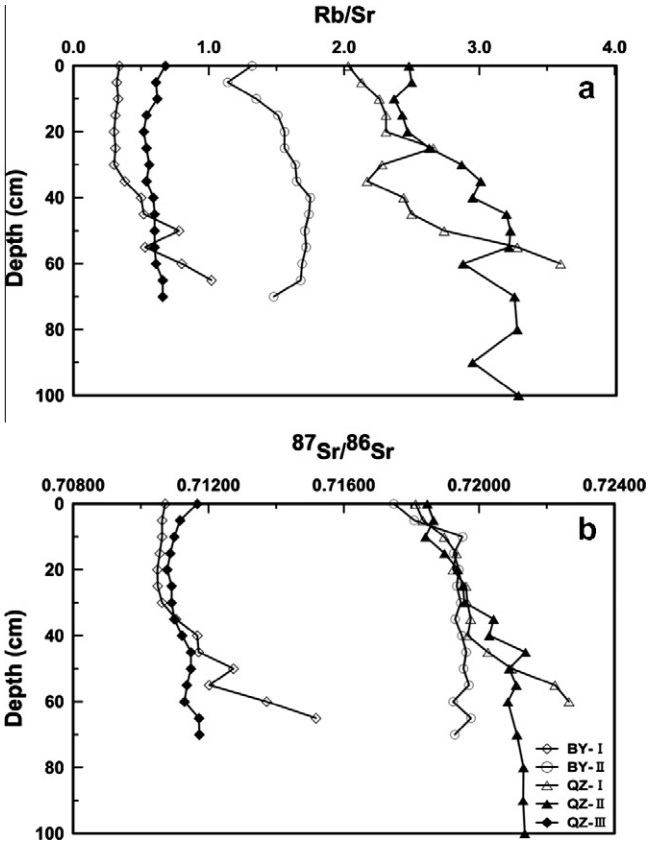

Fig. 2. Variations of Rb/Sr and $^{87}Sr/^{86}Sr$ ratios as a function of depth of the yellow sandstone soil profiles (BY-I and QZ-III) and limestone soil profiles (BY-II, QZ-I and QZ-II).

minerals change from smectite to kaolinite and gibbsite. The acid-insoluble residues of carbonate rocks are characterized by relatively high proportion of K_2O, implying dominance of K-feldspar and/or other K-containing minerals. The dominance of K-feldspar in the acid-insoluble residues is in according with the relatively high Rb/Sr (2.86) and $^{87}Sr/^{86}Sr$ ratio (0.747332) observed by Ji and Wang (2008) for the acid-insoluble material. In the A-CN-K and the A-CNK-FM ternary diagrams, several red residua samples show the highest Al_2O_3 value and relatively low FeO_T + MgO values, while the yellow soils developed on clastic rocks show the highest CaO^* + Na_2O and FeO_T + MgO values. As shown in Fig. 6, all of the limestone and sandstone soils, together with the red residua, show a general negative relationship between the CIA values and Na_2O/K_2O ratios, indicating that variation of Na_2O/K_2O ratio is also linked to the weathering intensity of the soils. Most of the limestone soils have lower Na_2O/K_2O but higher CIA values than the sandstone soils. The red residua show the highest CIA values and the lowest Na_2O/K_2O ratios, among all type of the soils considered. The limestone soils might have experienced more intense chemical weathering compared to the clastic rock soils, probably because the limestone soil was derived from further weathering of the accumulated clastic materials from dissolution of limestone.

5.1.2. Implications of Rb/Sr and $^{87}Sr/^{86}Sr$ ratio

Because of the similarity of ionic radii and equal electrovalence of the K–Rb and Ca–Sr pairs, Rb and Sr commonly substitute for K and Ca in K- and Ca-bearing minerals, respectively. K-feldspar is more resistant to weathering than plagioclase, and the former has a higher Rb/Sr and $^{87}Sr/^{86}Sr$ ratio than the latter (Goldich and Gast, 1966; Faure, 1986; Blum and Erel, 1997; Bullen et al., 1997). In addition, Sr and Ca are more readily leached by ambient solution, while K and Rb are more likely to be absorbed to the mineral surface, especially to the clay mineral surface (Nesbitt et al., 1980). Therefore, in a weathering profile, higher value of Rb/Sr ratio and radiogenic ^{87}Sr content indicate a higher extent of chemical weathering.

As displayed in Figs. 2 and 7, the limestone soils have higher Rb/Sr and $^{87}Sr/^{86}Sr$ ratios than the yellow sandstone soils, which probably indicates that the limestone soil contains more K-bearing minerals. However, the amount of weathering-resistant minerals in the limestone soils is not a direct indictor of weathering intensity of the soils, since the parent materials for the two types of soils are different. In general, the red residua, which show the highest $^{87}Sr/^{86}Sr$ ratios among all types of studied soils, is considered the products of intense weathering, however, their Rb/Sr ratios are not proportionally higher than the limestone and yellow sandstone soils, as shown in Fig. 7. The limestone soil profiles are developed on carbonate rocks, and the parent materials provided by carbonate dissolution would contain much clay mineral and/or detritus of fine-grain size if the limestone was formed in an open ocean or a relatively static environment. Accordingly, the limestone soils were formed through two processes or two stages: the first stage was the weathering of limestone and the second was the weathering of residual silicate detritus accumulated during the dissolution of carbonate rocks. The higher $^{87}Sr/^{86}Sr$ ratios of the limestone soil, as compared to those of the yellow sandstone soil, are in accordance with the higher Rb/Sr ratios, suggesting that a relatively long time elapsed after minerals sorting either by different gravity of minerals during transportation before carbonate deposition and/or by mineral weathering of different rates.

5.1.3. Implications of sequential leachate geochemistry

For a better understanding of weathering processes in the soil profiles, we have measured the Sr and Ca contents, along with the $^{87}Sr/^{86}Sr$ ratios of labile, carbonate, and residua (or silicate) fractions of the soil samples. The geochemical characteristics of labile phase are dominated by sorption/desorption processes, and

Table 3
Ca, Sr, Ca/Sr and $^{87}Sr/^{86}Sr$ ratio of leaching fractions of the soil samples in the studied profiles.

Sample	Labile				Carbonate				Silicate			
	Ca (μmol)	Sr (nmol)	Ca/Sr	$^{87}Sr/^{86}Sr$	Ca	Sr (nmol)	Ca/Sr	$^{87}Sr/^{86}Sr$	Ca	Sr (nmol)	Ca/Sr	$^{87}Sr/^{86}Sr$
Limestone soil												
BY-II (0–5)				0.70925				0.70927				
BY-II (10–15)	14.0	35.0	399	0.70936	5.10	11.1	461	0.70950	34.3	343	100	0.71946
BY-II (20–25)	24.2	48.0	504	0.70937	4.12	8.39	491	0.70962	21.5	313	69	0.72020
BY-II (30–35)	33.6	52.6	640	0.70942	3.78	8.96	422	0.70948	21.8	274	80	0.72012
BY-II (40–45)	35.1	55.6	631	0.70914	5.76	7.78	740	0.70964	25.6	309	83	0.72013
BY-II (50–55)	46.6	53.6	870	0.70901	5.22	8.97	582	0.70924	24.4	307	79	0.72037
BY-II (60–65)	45.4	53.3	851	0.70890	7.04	9.04	779	0.70905	20.8	298	70	0.72017
BY-II > 70	47.2	62.6	753	0.70862	6.88	9.78	704	0.70881	18.0	213	85	0.71998
QZ-I (0–5)	42.0	1456	288	0.70855	88.4	207	426	0.70832	13.7	324	42	0.72063
QZ-I (10–15)	38.4	111	346	0.70869	62.4	142	440	0.70877	12.2	301	40	0.72106
QZ-I (20–25)	78.8	115	688	0.70882	45.0	117	385	0.70880	12.3	312	39	0.72118
QZ-I (30–35)	42.0	85.1	493	0.70895	29.4	65.2	451	0.70904	10.2	191	53	
QZ-I (40–45)	29.2	68.0	429	0.70894	14.0	42.7	329	0.70901	8.97	248	36	0.72051
QZ-I (50–55)		73.7		0.70903		24.0		0.70900		250		0.72222
QZ-I (60–65)	27.1	60.4	448	0.70914	10.9	26.0	418	0.70926	7.72	181	43	0.72432
Yellow sandstone soil												
BY-I (10–15)	8.79	13.2	666	0.71251	8.94	4.47	2001	0.71271	9.45	514	18	0.71028
BY-I (20–25)	5.07	4.62	1096	0.71106	3.15	4.36	722		10.4	416	25	0.71023
BY-I (30–35)	4.59	3.64	1259	0.71125	2.43	3.31	734	0.71171	16.6	579	29	0.71022
BY-I (40–45)	4.50	5.41	832	0.71148	2.40	3.24	742		15.5	605	26	0.71087
BY-I (50–55)	7.50	9.62	780	0.71203	3.06	4.58	668		7.41	271	27	0.71155
BY-I (60–65)	9.36	7.41	1264	0.71138		3.93		0.71120	9.06	404	22	0.71161
BY-I >70	15.5	22.4	692	0.70946	7.53	10.2	738	0.70961	14.8	353	42	0.71450
QZ-III (0–5)	16.9	15.8	1068	0.70945	5.25	1.70	3088		12.5	806	15	0.71080
QZ-III (10–15)	8.25	6.84	1205	0.71031	3.51	6.36	552		13.0	650	20	0.71113
QZ-III (20–25)	6.72	7.71	872	0.71027	3.39	4.44	763	0.71066	9.87	625	16	0.71057
QZ-III (30–35)	5.88	8.07	729	0.71071	2.94	3.58	821	0.71098	10.2	562	18	0.71078
QZ-III (40–45)	4.26	8.33	512	0.71080	2.52	3.98	633	0.71101	8.10	506	16	0.71103
QZ-III (50–55)	4.29	7.22	594	0.71144	4.29	4.50	953	0.71226	10.4	645	16	0.71102
QZ-III (60–65)	5.64	6.57	859	0.71086	2.94	4.18	703		10.6	613	17	0.71135

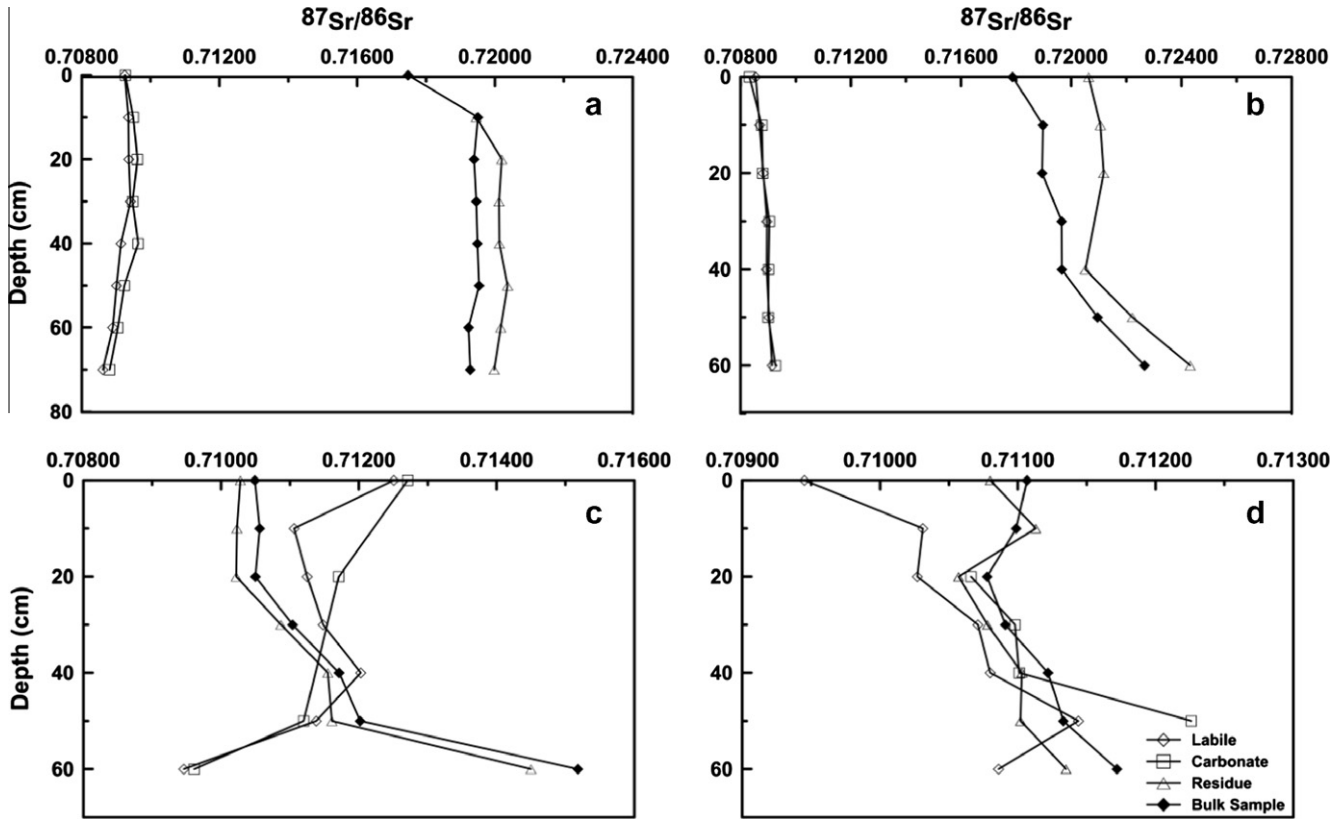

Fig. 3. Depth profiles of $^{87}Sr/^{86}Sr$ ratio of sequential extraction fractions and bulk samples from the yellow sandstone and limestone soil profiles. (a) BY-II; (b) QZ-I; (c) BY-I; (d) QZ-III.

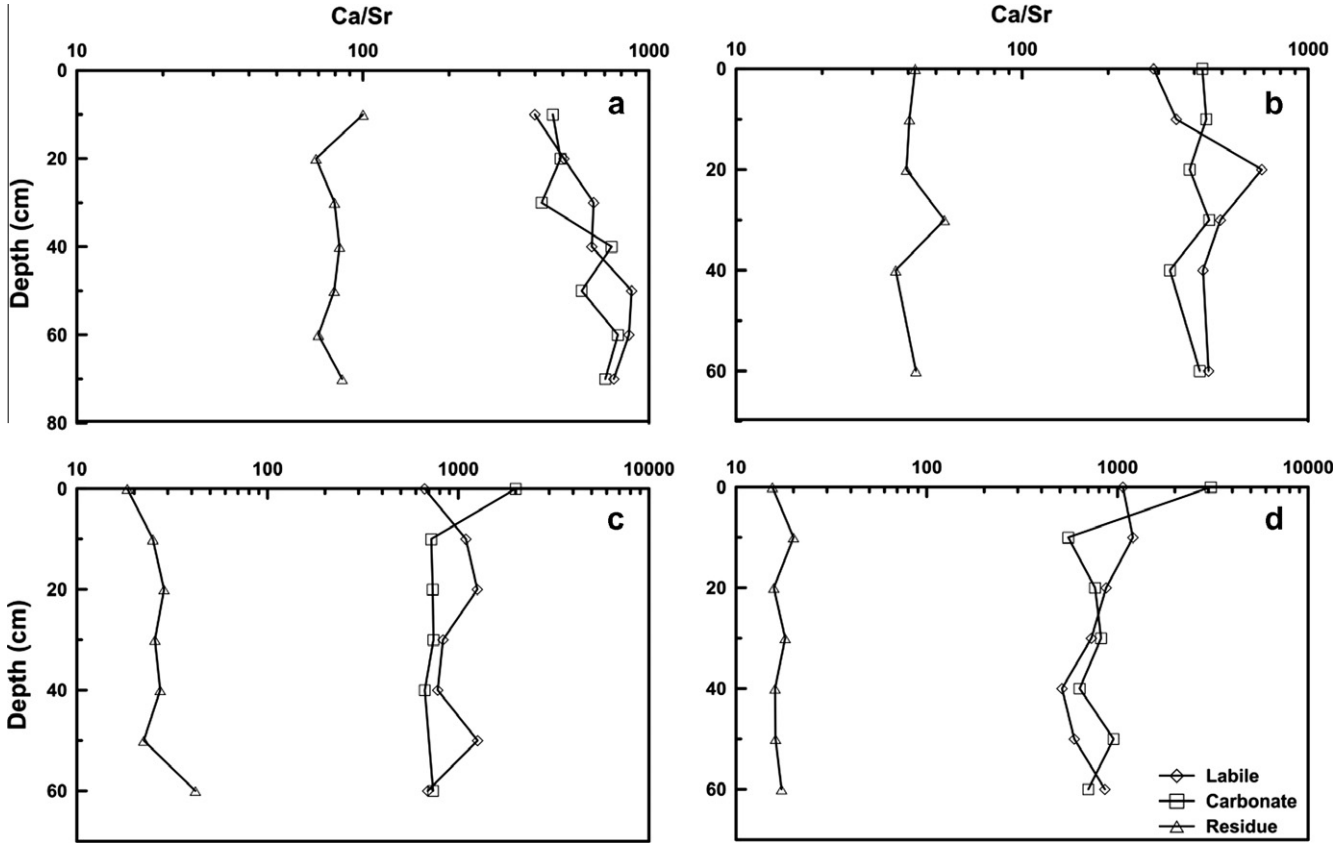

Fig. 4. Ca/Sr ratio in labile, carbonate and residue fraction of soil samples as a function of profile depth in yellow sandstone and limestone soil profile studied. (a) BY-II; (b) QZ-I; (c) BY-I; (d) QZ-III.

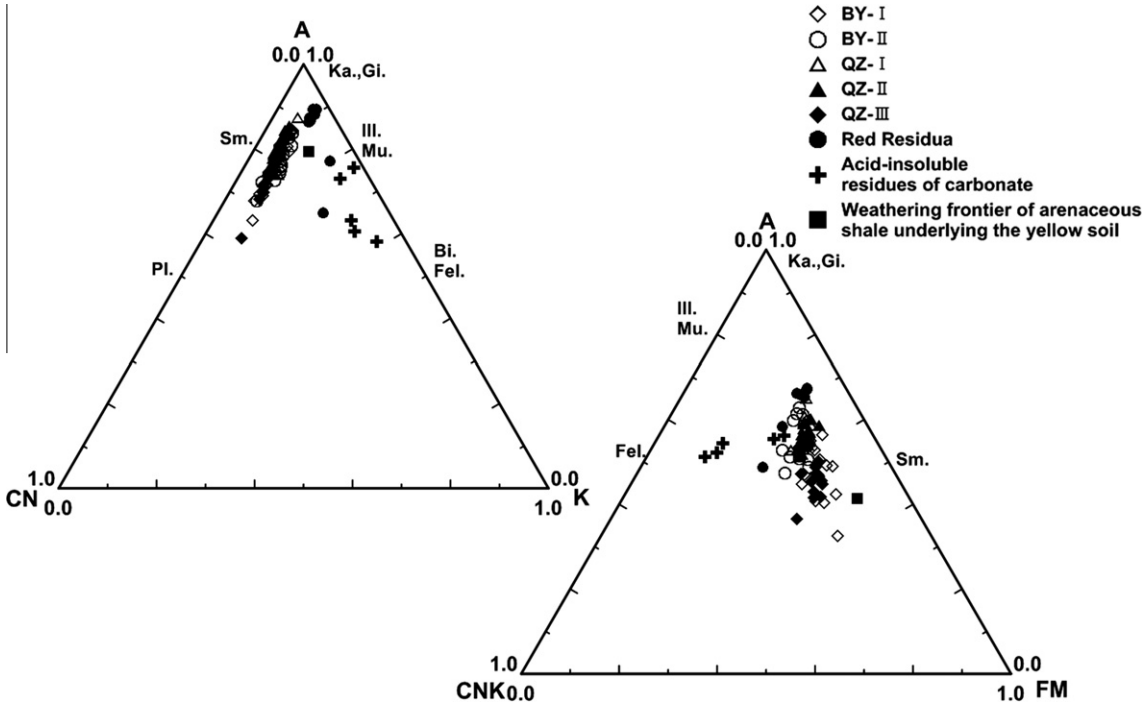

Fig. 5. A-CN-K and A-CNK-FM diagram of the yellow sandstone (BY-I and QZ-III) and limestone soil profiles (BY-II, QZ-I and QZ-II), red residua, acid-insoluble residues of carbonate, and the weathered bed rocks. Red residua data were cited from Sun et al. (2002); four data of acid-insoluble fraction of carbonate from Feng et al. (2002), Sun et al. (2002), and Wang et al. (2002).

the elements in the labile phase are derived from mineral weathering and atmospheric deposits (Harlavan et al., 2009). The carbonate phase is composed of pedogenic and non-pedogenic carbonate minerals (detrital limestone and marl particles from the vastly distributed carbonate rocks in karst area). The chemical components in the carbonate phase can be derived from the

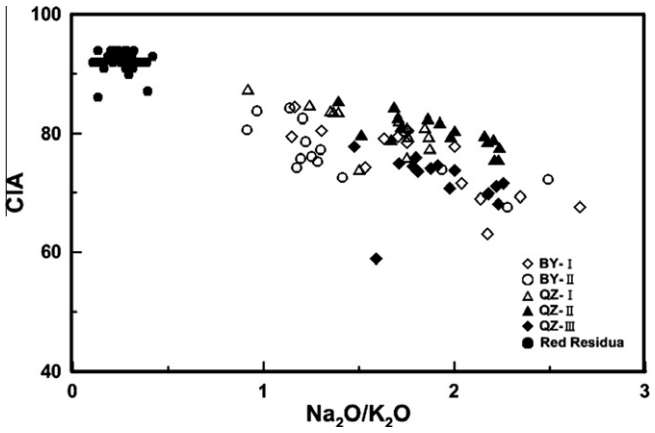

Fig. 6. Relationship between the CIA values and Na_2O/K_2O ratios for the yellow sandstone (BY-I and QZ-III) and limestone soil profiles (BY-II, QZ-I and QZ-II).

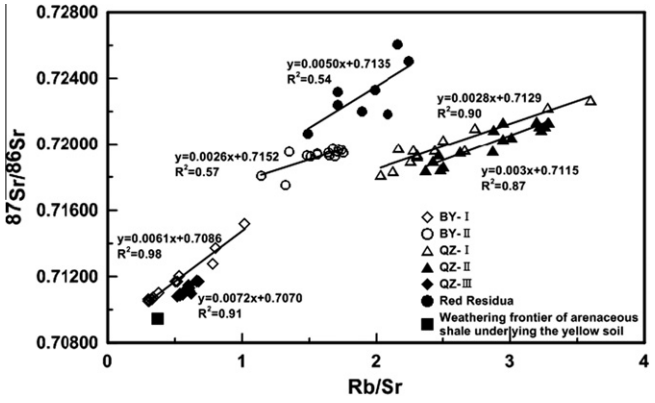

Fig. 7. Relationship between Rb/Sr and $^{87}Sr/^{86}Sr$ ratios of the samples from the yellow sandstone (BY-I and QZ-III) and limestone soil profiles (BY-II, QZ-I and QZ-II), as well as red residua profile. Red residua data were cited from Ji and Wang (2008).

dissolution of the detrital carbonate minerals (either from the bedrock or from the atmospheric dry deposition) and/or from the dissolution of secondary or pedogenic carbonate minerals, of which the chemical components in the pedogenic carbonate minerals may be derived from chemical weathering of both silicate and carbonate minerals (Chiquet et al., 1999). Accordingly, the chemical compositions of different phases in the soil profile are of different implications for chemical weathering of the soil.

The Ca and Sr contents of both labile and carbonate fractions in yellow sandstone soils are significantly lower than limestone soil. The Ca contents are slightly lower but the Sr contents much higher in the residue fraction of the yellow sandstone soils, as compared to the corresponding fractions of the limestone soils (Table 3). This is probably due to the higher soil pH values and more preservation of carbonate minerals of the limestone soils, and is because in the residue fraction of the yellow sandstone soil there are more Ca-containing silicate minerals. In general, the variations of the labile and carbonate Ca and Sr contents along the depth of the soil profiles are irregular, except for the profile QZ-I whose Ca and Sr contents of both labile and carbonate phase decrease with increasing soil profile depth. As shown in Fig. 4, Ca/Sr ratios in both labile and carbonate fractions are higher than those in the residue fractions of all soil profiles, which would be due to preferential releasing and transportation of Ca and retention of Sr in soil, since there is a slightly stronger affinity of Sr for ion exchange sites than Ca during the leaching process (Bruggenwert and Kamphorst, 1979; Sposito, 2008). The fractionation values $[(Ca/Sr)_{labile\ or\ carbonate}/(Ca/Sr)_{residue}]$ of Ca and Sr between labile, carbonate and residue are larger in yellow sandstone soil than in limestone soil, which could be ascribed to the different mineral compositions and ambient physical and chemical features of the two kinds of soil. The depth profile of Ca/Sr ratios show different and variable patterns for labile and carbonate fractions in different soil profiles, which cannot be interpreted simply in terms of single factor. In addition, Ca is an essential plant nutrient, with a great demand in the process of vegetation growing, while Sr is of little significance itself as a nutrient (Capo et al., 1998). Accordingly, Ca/Sr ratios may be fractionated during plant uptake or allocation (Pett-Ridge et al., 2009), in addition to fractionation due to different chemical behavior of these two elements in the chemical weathering process.

Fig. 8 displays the $^{87}Sr/^{86}Sr$ variations with Ca/Sr ratios in the labile (Fig. 8a), carbonate (Fig. 8b), and residual (Fig. 8c) phases of sandstone and limestone soils. $^{87}Sr/^{86}Sr$ ratio is not changed by adsorption or precipitation processes in weathering or preferential uptake by plants and therefore provides a useful tool for verifying the source of Sr and Ca and for tracing mineral weathering reaction

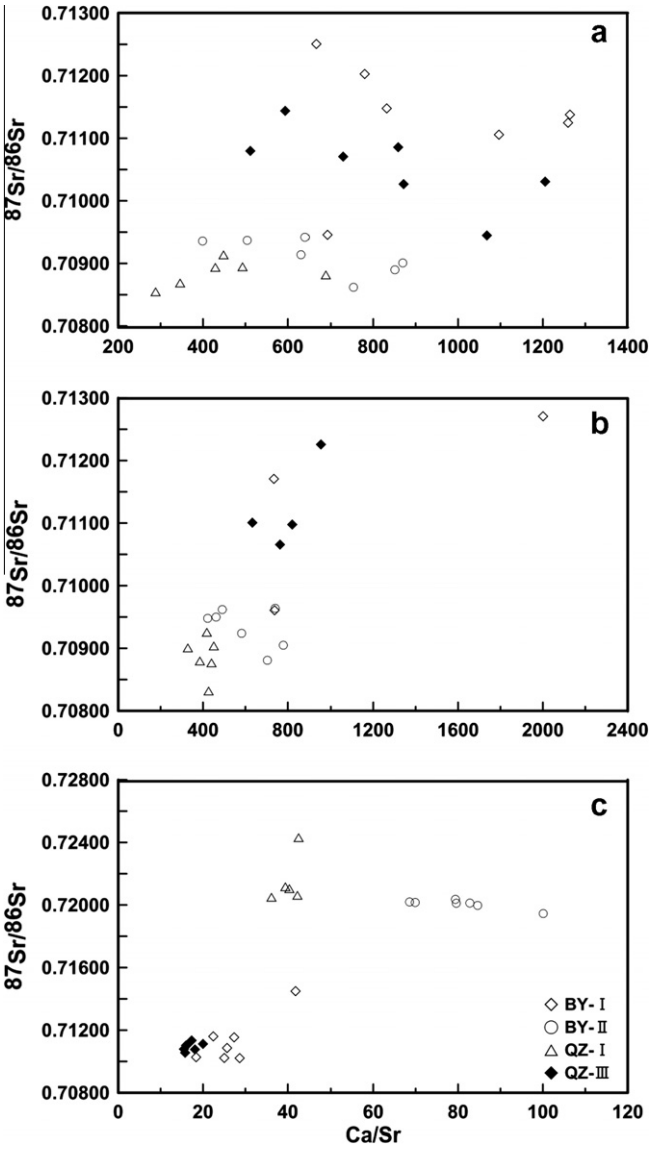

Fig. 8. Ca/Sr plotted against $^{87}Sr/^{86}Sr$ ratio of labile (a), carbonate (b), and residue (c) fraction of samples from the yellow sandstone (BY-I and QZ-III) and limestone soil profiles (BY-II, QZ-I and QZ-II).

(Blum and Erel, 1997; Jacobson et al., 2002). Of limestone soils, the labile and carbonate phases of these soils have much lower $^{87}Sr/^{86}Sr$ ratios than the silicate phase, which suggests that major part of Sr in these two phases was derived from detrital carbonate minerals. Unlike the limestone soils, the yellow sandstone soils have similar $^{87}Sr/^{86}Sr$ ratios in carbonate, labile and silicate phase, which indicates that the Sr in the labile and carbonate phases was derived mainly from silicate weathering in the yellow sandstone soils (Fig. 3).

5.1.4. Contribution of atmospheric Sr to the carbonate and labile fractions of the soils

A general binary mixing trend can be observed for the labile Sr in these two sandstone soil profiles (Fig. 8a), which suggests that the labile Sr in the sandstone soils could be derived mainly from two sources: one was silicate weathering origin, which had high Sr isotope and low Ca/Sr ratios; another was carbonate weathering and/or atmospheric origin, since the atmospheric Sr often show similar $^{87}Sr/^{86}Sr$ ratios to carbonate. Atmospheric precipitation and mineral weathering are the two possible sources of Sr in the labile and carbonate fractions of weathering profiles. The atmospheric Sr precipitates to the surface of the soil, and penetrates into the deep part of the profile, leading to a vertical distribution grads of the labile Sr isotopic composition (Wickman and Jacks, 1993; Dambrine et al., 1997). Han (2005) reported the $^{87}Sr/^{86}Sr$ ratios of rainwater collected at Guiyang, in the range of 0.707934–0.709080, averaging on 0.708219, and concluded that the Sr in rain water had been derived from both anthropogenic inputs and natural carbonate dissolution. The $^{87}Sr/^{86}Sr$ ratio of anthropogenic Sr is 0.7080 in Guizhou province, as estimated according to the study of Sr isotope composition of Wujiang river water by Han and Liu (2004). Vilomet et al. (2001) gave the $^{87}Sr/^{86}Sr$ ratio of landfill leachate at 0.708457. The strontium isotope composition of fertilizer was reported to be 0.7079–0.7087 (Négrel and Deschamps, 1996). The $^{87}Sr/^{86}Sr$ ratio for automobile exhaust was reported to be 0.7077–0.7083 (Négrel et al., 2007). These different estimates of anthropogenic Sr in the previous studies show $^{87}Sr/^{86}Sr$ ratios close to that of Triassic carbonate (0.70775) in the karst area of southwest China. These complicate the identification of atmospheric and carbonate Sr in the soils. Fig. 9a illustrates the $^{87}Sr/^{86}Sr$ variations with 1/Sr values of the bulk soil, which does not show a binary mixing relationship simply between two sources for the soil profile, with the exception of the soil profile QZ-I, which shows a general increase in the $^{87}Sr/^{86}Sr$ ratio with increasing 1/Sr value. Sr in bulk soils generally exists in three phases, which are silicate, carbonate, and adsorbed forms. The Sr of the adsorbed form can be further sub-grouped into three types in origin, atmospheric, silicate and carbonate weathering. The mixing relationship of Sr in the bulk soil of the soil profile QZ-I, if really exists, can be ascribed to mixing of carbonate and silicate Sr. However, as to carbonate fraction, the samples from the two limestone soil profiles hold a general two-end member mixing pattern, while the yellow sandstone soil samples display a complicate mixing pattern of multiple end members (Fig. 9b).

5.1.5. Vertical variation of weathering indices along the soil profiles

Fig. 10 shows the vertical variations of CIA values and Na_2O/K_2O ratios of the studied soil profiles, all of which do not show a simple increasing or decreasing pattern along the soil profiles. For the limestone soil profiles, the CIA values are not largely variable, and generally decrease from the 30 cm depth to the top soil, but are constant below 30 cm depth. The two sandstone soil profiles show different variation patterns of the CIA values. The soil profile BY-I shows increasing CIA values from 15 cm depth to the top soil, but decreasing CIA values from 45 cm depth to the 15 cm depth of the soil profile. The soil profile QZ-III shows a general increase of

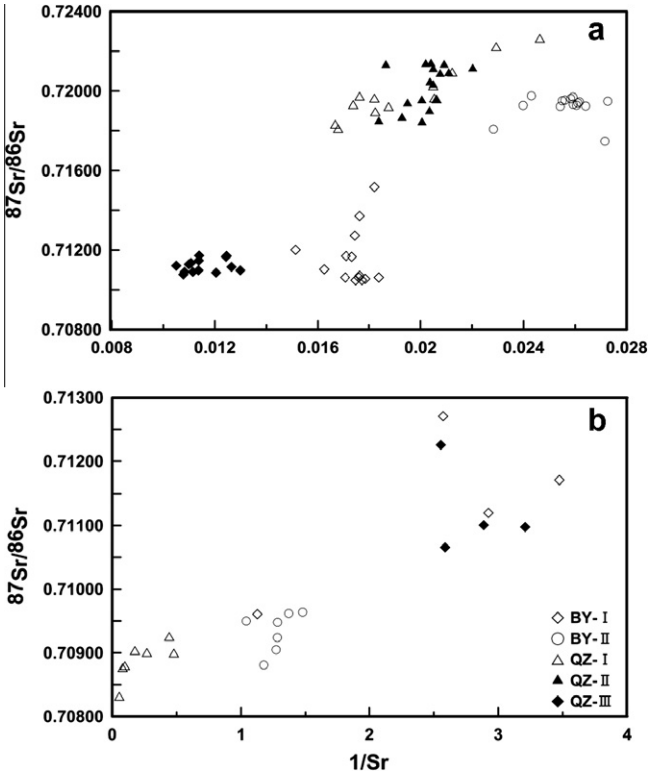

Fig. 9. Relationship between soil $^{87}Sr/^{86}Sr$ ratios and 1/Sr $(mg/L)^{-1}$ of the bulk samples (a) and carbonate fraction (b) of the yellow sandstone (BY-I and QZ-III) and limestone soil profiles (BY-II, QZ-I and QZ-II).

the CIA values from deeper to the top soil, with one sample at 35 cm depth has an exceptionally lower CIA value. The depth profiles of the Na_2O/K_2O and Na_2O/Al_2O_3 ratios for the two types of the soil profiles are of similar variation trends. The Na_2O/K_2O and Na_2O/Al_2O_3 ratios do not vary largely and regularly along the limestone soil profiles, and are relatively constant along the soil profiles. Like the CIA depth profiles, the depth profiles of the Na_2O/K_2O and Na_2O/Al_2O_3 ratios of the two sandstone soil profiles are different: the soil profile BY-I shows more variability and irregular variation pattern, while the soil profile QZ-III displays a general decrease in both Na_2O/K_2O and Na_2O/Al_2O_3 ratios from the bottom to the top of the profile. The depth profiles of the Rb/Sr and $^{87}Sr/^{86}Sr$ ratios of the soil profiles developed on both limestone and sandstone show a tendency of increasing Rb/Sr and $^{87}Sr/^{86}Sr$ ratio with increasing depth of soil profile (Table 2, Fig. 2). Along with the depth profiles of the weathering indices CIA value, the Na_2O/K_2O and Na_2O/Al_2O_3 ratios, the depth profiles of all the weathering intensity indices considered here show different patterns from those of the in situ weathering profiles (Blum and Erel, 1995; Ma et al., 2010), which have variation trends of the weathering intensity indices showing higher weathering intensity of the upper and lower intensity of lower part of the weathering profile. There are probably four mechanisms responsible for this depth-dependent variation of weathering intensity. The first mechanism is that the soil profiles, especially the limestone soil profiles, were formed through accumulation of residual materials from carbonate rock dissolution and then in situ chemical weathering of the accumulated deposits. This formation process of the limestone soils might have produced a weathering soil profile with higher weathering intensity at the top and lower intensity at the deep part of the soil profile. The second mechanism is that biological process or activities of macro- and microorganisms in the deeper soil intensify the soil weathering, since the deepest soils

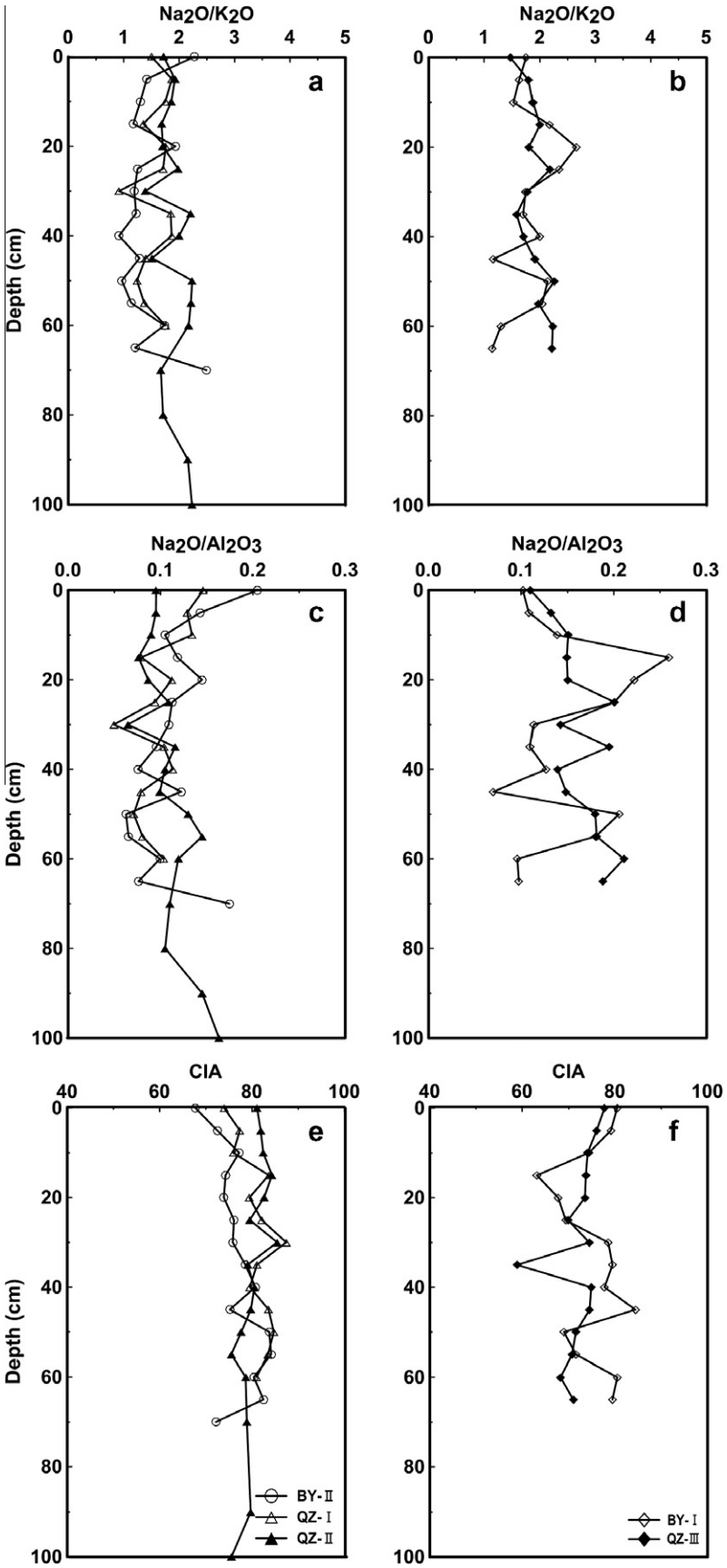

Fig. 10. Vertical variations of CIA values, Na_2O/Al_2O_3 and Na_2O/K_2O ratios of the soil profiles. Diagrams (a), (c), and (e) are for the limestone soil profiles (BY-II, QZ-I and QZ-II), while the diagrams (b), (d), and (f) for the sandstone soil profiles (BY-I and QZ-III).

collected in this study is at the depth where the organisms could be active. The third mechanism is the leaching of minerals with fine grain size, such as clay minerals, from upper part to lower part of the soil profiles, which would result in an increase of Rb/Sr, Na_2O/Al_2O_3 ratios and CIA values for the soil at lower part of the soil profiles. This mechanism is probably responsible for both the lower CIA values and Na_2O/K_2O ratios, but higher Na_2O/Al_2O_3 ratios in the top soil of the soil profiles. The last mechanism probably involves external inputs most likely from atmospheric deposition and also from upper land. Atmosphere precipitation, along with mineral weathering, is one of potential sources for Sr and also other elements in the weathering profiles. The atmospheric Sr precipitates to the surface of the soil, and penetrates into the deeper part of the profile, leading to a vertical distribution grads of the labile Sr isotopic composition (Wickman and Jacks, 1993; Dambrine et al., 1997). Rainwater in Guiyang has its Sr content at 0.02–0.33 μmol/L, and $^{87}Sr/^{86}Sr$ ratio at 0.70793–0.70908 (Han and Liu, 2004), lower than all the samples. Accordingly, the introduction of rain-originated Sr into the soil may lead to a decrease in $^{87}Sr/^{86}Sr$ ratio of both labile fraction and the bulk soils especially at the top part of the soil profiles. Above all, it is difficult to exactly tell the importance of individual mechanism for producing such a Sr isotopic tendency in a weathering soil profile. However, the similar $^{87}Sr/^{86}Sr$ ratios of the residue fraction and the bulk samples and also the coherent values between the labile and carbonate fraction of the sample imply that multi-stage formation processes, especially the accumulation and the following weathering of the accumulated residua from carbonate weathering would be the main mechanism giving rise to the weathering signature of the limestone soil. In a comprehensive perspective, it is quite possible that all of the considered mechanisms worked together to generate the depth profiles of the weathering indices such as $^{87}Sr/^{86}Sr$, Rb/Sr, Na_2O/Al_2O_3 ratios, and CIA values of the soils.

5.2. The source materials of the soils

5.2.1. Constraints from Rb/Sr ratio and Sr isotopic composition

Previous studies of weathering profiles indicate that suites of weathered rocks form linear arrays on the isochron diagram whose slopes yield dates that are younger than the age of the rocks (Faure, 1986). The Rb-bearing minerals (mainly micas and K-feldspar) are more resistant than the Ca (and Sr)-bearing minerals (mainly plagioclase and calcite) during chemical weathering (Faure, 1986), and so the weathering generally leads to the fractionation between Rb and Sr and also to the different leaching rates of common ^{87}Sr and radiogenic ^{87}Sr (Clauer, 1981). As a result, both Rb/Sr and $^{87}Sr/^{86}Sr$ ratios of the soil profile samples tend to increase with increasing weathering intensity. In the case of little external disturbance, the decomposition of Rb-bearing minerals will lead to contemporaneous loss of both Rb and ^{87}Sr from the weathering profiles, hence resulting in a better positive correlation between Rb/Sr and $^{87}Sr/^{86}Sr$ ratios (Ma and Liu, 2001).

In this study, we focus on the characterization of weathering process and identification of parental materials of the yellow sandstone soil, limestone soil, and the red residua, rather than the age information shown by the relationship between Rb/Sr and $^{87}Sr/^{86}Sr$ ratios. Fig. 7 shows the variations of $^{87}Sr/^{86}Sr$ with Rb/Sr ratios for the soil profiles, and each soil profile individually shows a generally good positive relationship. The slopes of the trend lines indicate the different mineralogical compositions and relative contents of Rb and Sr in the samples from each profile, while the selective adsorption of Rb and Sr onto clays results in deviations from the line (Ma et al., 2004). The samples from the two yellow sandstone soil profiles share close slopes (0.0061 and 0.0072) and intercepts (0.7086 and 0.7070) on the $^{87}Sr/^{86}Sr$ axis, and have much lower Rb/Sr and $^{87}Sr/^{86}Sr$ ratios than the limestone soils and the red residua, though these two soil profiles are located far from each other. The slightly weathered rock sample collected from the soil profile BY-I is arenaceous shale, and holds relatively lower $^{87}Sr/^{86}Sr$ (0.70943) and Rb/Sr ratio (0.37) than overlying soils, which imply that the weathering of rocks gave rise to both higher Rb/Sr and $^{87}Sr/^{86}Sr$ ratios of the weathering products as compared to the parent rocks. All of the limestone soil profiles show similar $^{87}Sr/^{86}Sr$ ratios, slopes (0.0026–0.003) of the trend lines, and the intercepts (0.7115–0.7152) on the $^{87}Sr/^{86}Sr$ axis, but show variable Rb/Sr abundance ratios. The red residua samples studied by Ji and Wang (2008) have the highest $^{87}Sr/^{86}Sr$ ratios, but median trend-line slope (0.005) and intercept (0.7135) between those of the yellow sandstone soils and the yellow limestone soils. The high $^{87}Sr/^{86}Sr$ ratios of the red residua may be ascribed to high Rb/Sr ratio, or old age, or differentiation of minerals during weathering processes, or all of these factors together.

The acid-insoluble residues of carbonate rock underlying the red residua has Rb/Sr ratio at 2.86 and $^{87}Sr/^{86}Sr$ ratio 0.747332 (Ji and Wang, 2008), much higher than both ratios of the red residua (Rb/Sr = 1.49–2.25, $^{87}Sr/^{86}Sr$ = 0.720657–0.726073). We have also measured one sample of acid-insoluble residues from the dissolution of the limestone underlying the limestone soil profile QZ-I. This acid-insoluble residue sample has Rb/Sr ratio at 7.11 and $^{87}Sr/^{86}Sr$ ratio 0.780441, largely higher than those (Rb/Sr = 2.03–3.60, $^{87}Sr/^{86}Sr$ = 0.71812–0.72266) of the bulk samples of the soils, and also higher than $^{87}Sr/^{86}Sr$ ratios ($^{87}Sr/^{86}Sr$ = 0.72063–0.72432) of the silicate fraction of the soil profile. The higher Rb/Sr and $^{87}Sr/^{86}Sr$ ratios of the acid-insoluble residues suggest that the overlying soil profiles and red residua developed on carbonate rocks, unlike the soil profiles developed on the sandstone rocks, did not totally inherited parent materials from the underlying rocks, because weathering of acid-soluble residues of the carbonate rocks should have resulted in higher Rb/Sr and $^{87}Sr/^{86}Sr$ ratios in the weathering profiles. Combined with the main lithology and geomorphology in the studied area and the possible parental material discussed in the trace element session below, the Rb/Sr and Sr isotope ratios of the soil profiles suggest that the red residua and even the limestone soils would be formed from chemical weathering of mixed materials mainly derived from both limestone and sandstone weathering.

5.2.2. Constraints from trace element composition

Zr and Hf exist mainly in the same minerals, like zircon and baddeleyite, and Nb in columbite, tantalite and Ti-bearing mineral rutile. All Zr- and Hf- and Nb-bearing minerals are normally resistant to chemical weathering. Even when the parent material is subject to extreme alteration, all of these three elements are particularly immobile in the earth's surface environment and enriched in the weathering residua due to their high ionic field strength and considerably low solubility in natural water (Middelburg et al., 1988; Bonjour and Dabard, 1991; Maynard, 1992). The Zr/Nb and Hf/Nb ratios are not sensitive to weathering and soil formation processes and can therefore be used to study the provenance of deposits. Therefore, these elemental ratios as provenance tracers are adopted here to discuss the origin or geochemical features of the limestone and yellow sandstone soils.

The Zr/Nb and Hf/Nb ratios of the limestone and yellow sandstone soil profiles, together with those of red residua and potential parent materials in the study areas, are displayed in Fig. 11. As shown in the figure, the different soils are characterized by specific Zr/Nb and Hf/Nb ratios: the limestone soils have the highest while the yellow sandstone soils the lowest Zr/Nb and Hf/Nb ratios, and the red residua have the ratios between those of the former two types of soils. The acid-insoluble materials of both limestone and dolomite rocks show the Zr/Nb and Hf/Nb ratios similar to those of the limestone soils. The Zr/Nb and Hf/Nb ratios displayed in

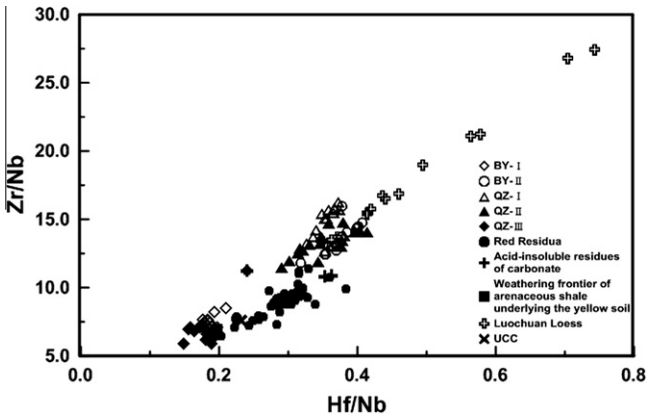

Fig. 11. Plot of Hf/Nb versus Zr/Nb ratio of samples from the yellow sandstone (BY - I and QZ-III) and limestone soil profiles (BY-II, QZ-I and QZ-II), red residua profiles and acid-insoluble residues of carbonate, and the weathered clastic bed rock. The data of red residua are from Huaxi (Sun et al., 2002); Jishou (Wang et al., 2002), Xinpu (Ji et al., 1999) and Pingba (Ji et al., 2004); the loess data from Gallet et al. (1996); the dilute acid-insoluble residues of carbonate in the areas studied are reported in previous work by Ji et al.(1999, 2004), and Wang et al. (2007).

Fig. 11 distinguish the different types of soils from each other, indicating different geochemical signatures of the parent materials for the different types of the soils.

As mentioned in the introduction section, the origin of the thick and widely distributed yellow or reddish-yellow soil layer or mantle developed on carbonate rocks, also called red residua or terra rossa, remain controversial as regard to its parent materials. Up to now, there have beenat least six theories regarding the origin of the red residua (reviewed by Feng et al., 2009b), among which the key debate focuses on source of soil parent materials and formation process. The Zr/Nb and Hf/Nb ratios of the red residua, which are higher than those of the soils developed from silicate rocks and lower than those of soils developed from carbonate rocks, strongly argue against single-source origin either from carbonate rock weathering or silicate clastic rocks, and hence also against in situ weathering of carbonate or silicate rocks.

It is demonstrated here by the geochemistry of inactive elements that the materials forming the red residua are the mixture of weathering products of both limestone and silicate clastic rocks. Carbonate rocks are widely distributed and interbeded with Permian silicate clastic rocks in most of areas SW China. In addition, a large amount of accumulation of residua from weathering of carbonate rocks hardly takes place since the silicate clastic materials in carbonate rocks are quite few. Therefore, both the trace element geochemistry and the geological setting of the karst terrains support the conclusion that the widely distributed red residua was formed through weathering of carbonate weathering residua as well as silicate clastic rocks.

The yellow sandstone soil samples have Zr/Nb and Hf/Nb ratios similar to those of the weathered sandstone or arenaceous shale, and also to the average ratios of the upper continental crust (UCC), showing the origin of the yellow sandstone soil from weathering of the underlying rocks. The Zr/Nb and Hf/Nb ratios of the acid-insoluble materials are similar to, but slightly lower than those of the limestone soils, suggesting that the limestone soils, including both of black limestone soil and yellow limestone soil, probably developed mainly from the acid-insoluble materials of the limestone. Since all of the Zr/Nb and Hf/Nb ratio data for the acid-insoluble materials of carbonate rocks are lower than those of the limestone soils, it is reasonable to think that there probably exists a type of materials with higher Zr/Nb and Hf/Nb ratios than the limestone soil, which is needed to account for the higher Zr/Nb and Hf/Nb ratios of the limestone soil compared to other kinds of profile and possible source materials here. We plotted the Zr/Nb and Hf/Nb ratios of loess collected from the Luochuan loess profile into Fig. 11, because some authors (Syers et al., 1969; Macleod, 1980; Mee et al., 2004) suggested an eolian theory for the origin of the red residua. The loess has generally the highest but variable Zr/Nb and Hf/Nb ratios, as displayed in Fig. 11, which implies that the eolian mineral dust also could be one type of parent materials for all soil types considered here. However, it is not mature to make a conclusion whether or not the source materials of the red residual and limestone soils are also of eolian origin, since much systematic work is necessary to verify the contribution of eolian dust materials to the formation of the soils in the karst region.

6. Conclusion

In terms of major chemical composition, the A-CN-K and A-CNK-FM ternary compositions of the soils suggest that all the sandstone and limestone soils are developing a stage at which feldspar is exhausting and the clay minerals are changing from smectite to kaolinite and gibbsite. The depth profiles of CIA values, Na_2O/Al_2O_3, Na_2O/K_2O, Rb/Sr concentration ratios and $^{87}Sr/^{86}Sr$ isotopic ratios demonstrate that the sandstone and limestone soil profiles investigated are the products of multiple stages or processes, that is, accumulation and weathering of the weathering residua of carbonate rocks and inputted external detrital materials, followed by pedogenesis. The Ca/Sr ratios in both labile and carbonate fractions are higher than those in the residue fractions of all soil profiles, which would be due to preferential releasing and transportation of Ca and retention of Sr in the soil. The fractionation values $[(Ca/Sr)_{labile\ or\ carbonate}/(Ca/Sr)_{residue}]$ of Ca and Sr between labile as well as carbonate and residue are larger in yellow sandstone than in limestone soil, most likely as a result of different mineral composition and weathering extent.

The immobile trace elemental pairs, Hf/Nb and Zr/Nb ratios, divide the yellow sandstone soil, limestone soil and the red residua into obviously different groups, indicating that their parent materials are distinct. This is further supported by the Rb/Sr and $^{87}Sr/^{86}Sr$ ratios of bulk sample and residue fraction. Both the trace element geochemistry and the geology setting of the karst terrains support that both carbonate and silicate clastic rocks served as the parent materials of the widely distributed red residua, and also the limestone soils.

Acknowledgements

We thank the two anonymous reviewers for their constructive reviews. This work was financially supported by the National Natural Science Foundation and Ministry of Science and Technology, China (Grants Nos. 41130536, 2013CB956700, 41021062).

References

Blum, J.D., Erel, Y., 1995. A silicate weathering mechanism linking increases in marine $^{87}Sr/^{86}Sr$ with global glaciation. Nature 373 (6513), 415–418.

Blum, J.D., Erel, Y., 1997. Rb-Sr isotope systematics of a granitic soil chronosequence: the importance of biotite weathering. Geochim. Cosmochim. Acta 61 (15), 3193–3204.

Bonjour, J.L., Dabard, M.P., 1991. Ti/Nb ratios of clastic terrigenous sediments used as an indicator of provenance. Chem. Geol. 91 (3), 257–267.

Bruggenwert, M.G.M., Kamphorst, A., 1979. Survey of experimental information on cation exchange in soil systems. Dev. Soil Sci. 5 (B), 141–203.

Bullen, T., White, A., Blum, A., et al., 1997. Chemical weathering of a soil chronosequence on granitoid alluvium: II. Mineralogic and isotopic constraints on the behavior of strontium. Geochim. Cosmochim. Acta 61 (2), 291–306.

Capo, R.C., Stewart, B.W., Chadwick, O.A., 1998. Strontium isotopes as tracers of ecosystem processes: theory and methods. Geoderma 82 (1–3), 197–225.

Chiquet, A., Michard, A., Nahon, D., et al., 1999. Atmospheric input vs in situ weathering in the genesis of calcretes: an Sr isotope study at Gávez (Central Spain). Geochim. Cosmochim. Acta 63 (3–4), 311–323.

Clauer, N., 1981. Strontium and argon isotopes in naturally weathered biotites, muscovites and feldspars. Chem. Geol. 31, 325–334.
Clow, D.W., Mast, M.A., 2010. Mechanisms for chemostatic behavior in catchments: implications for CO_2 consumption by mineral weathering. Chem. Geol. 269 (1–2), 40–51.
Cooke, M.J., Stern, L.A., Banner, J.L., et al., 2007. Evidence for the silicate source of relict soils on the Edwards Plateau, central Texas. Quat. Res. 67 (2), 275–285.
Dambrine, E., Loubet, M., Vega, J.A., et al., 1997. Localisation of mineral uptake by roots using Sr isotopes. Plant Soil 192 (1), 129–132.
Dessert, C., Dupré, B., Gaillardet, J., et al., 2003. Basalt weathering laws and the impact of basalt weathering on the global carbon cycle. Chem. Geol. 202 (3–4), 257–273.
Driese, S.G., Jacobs, J.R., Nordt, L.C., 2003. Comparison of modern and ancient Vertisols developed on limestone in terms of their geochemistry and parent material. Sediment. Geol. 157 (1–2), 49–69.
Durn, G., Ottner, F., Slovenec, D., 1999. Mineralogical and geochemical indicators of the polygenetic nature of terra rossa in Istria. Croatia. Geoderma 91 (1–2), 125–150.
Faure, G., 1986. Principles of Isotope Geology. Wiley & John, Ltd., New York, 589 pp.
Feng, J., Cui, Z., Zhu, L., 2009a. Origin of terra rossa over dolomite on the Yunnan-Guizhou Plateau, China. Geochem. J. 43 (3), 151–166.
Feng, J., Zhu, L., 2009. Origin of terra rossa on Amdo North Mountain on the Tibetan plateau, China: evidence from quartz. Soil Sci. Plant Nutr. 55 (3), 407–420.
Feng, J., Zhu, L., Cui, Z., 2009b. Quartz features constrain the origin of terra rossa over dolomite on the Yunnan-Guizhou Plateau, China. J. Asian Earth Sci. 36 (2–3), 156–167.
Feng, Z., Wang, S., Sun, C., 2002. Discussion on possible causes of increases in Si/Al ratio in surface layers of some lateritic profiles. Geol. Geochem. 30 (4), 7–14 (in Chinese with English abstract).
Gallet, S., Jahn, B., Torii, M., 1996. Geochemical characterization of the Luochuan loess-paleosol sequence, China, and paleoclimatic implications. Chem. Geol. 133, 67–88.
Goldich, S.S., Gast, P.W., 1966. Effects of weathering on the Rb-Sr and K-Ar ages of biotite from the Morton Gneiss, Minnesota. Earth Planet. Sci. Lett. 1 (6), 372–375.
Hall, R.D., 1976. Stratigraphy and origin of surficial deposits in sinkholes in south-central Indiana. Geology 4 (8), 507–509.
Han, G., Liu, C., 2004. Water geochemistry controlled by carbonate dissolution: a study of the river waters draining karst-dominated terrain, Guizhou Province, China. Chem. Geol. 204 (1–2), 1–21.
Han, G., Liu, C., 2005. Strontium isotope and major ion chemistry of the raiwaters from Guiyang, Guizhou provice, China. Environ. Chem. 24 (2), 213–218 (in Chinese with English abstract).
Harlavan, Y., Erel, Y., Blum, J.D., 2009. The coupled release of REE and Pb to the soil labile pool with time by weathering of accessory phases, Wind River Mountains, WY. Geochim. Cosmochim. Acta 73 (2), 320–336.
Jackson, M.L., 1982. Eolian influence on terra rossa soils of Italy traced buy quartz oxygen isotope ratio. Int. Clay Conf. 1981, 293–301.
Jacobson, A.D., Blum, J.D., Chamberlain, C.P., et al., 2002. Ca/Sr and Sr isotope systematics of a Himalayan glacial chronosequence: carbonate versus silicate weathering rates as a function of landscape surface age. Geochim. Cosmochim. Acta 66 (1), 13–27.
Ji, H., Ouyang, Z., Wang, S., et al., 1999. Elemental geochemistry characteristics of a dolomite weathering profile in the northern Guizhou province and its implication for upper crustal composition. Sci. China Ser. D 29 (6), 504–513 (in Chinese).
Ji, H., Wang, S., 2008. Sr-Nd isotope composition and evolution in a dolomite weathering profile in the central Guizhou province Prog. Nat. Sci. 18 (10), 1128–1135 (in Chinese).
Ji, H., Wang, S., Ouyang, Z., et al., 2004. Geochemistry of red residua underlying dolomites in karst terrains of Yunnan-Guizhou Plateau: I. The formation of the Pingba profile. Chem. Geol. 203 (1–2), 1–27.
Kirschbaum, A., Martínez, E., Pettinari, G., et al., 2005. Weathering profiles in granites, Sierra Norte (Córdoba, Argentina). J. S. Am. Earth. Sci. 19 (4), 479–493.
Kronberg, B.I., Nesbitt, H.W., Fyfe, W.S., 1987. Mobilities of alkalis, alkaline earths and halogens during weathering. Chem. Geol. 60 (1–4), 41–49.
Li, J.Y., Wang, C.F., 1988. Comment on karst geological processes and karst environment. Research on Karst Environment in Guizhou Province. People Press of Guizhou (in Chinese).
Liu, C., 2009. Biogeochemical Processes and Cycling of Nutriens in the Earth's Surface: Cycling of Nutrients in Soi-Plant Systems of Karstic Environments South west China. Science Publishing Company, Beijing, 618 pp (in Chinese).
Liu, S., Zhang, M., 1997. Regional Soil Geography. Press of Sichuan University, Chengdu, 357 pp (in Chinese).
Liu, X., Wang, S., Feng, Z., et al., 2004. Identification of origin of limestone soil-case study of profiles in central and north Guizhou. Soils 36 (1), 30–36 (in Chinese with English abstract).
Ma, J., Wei, G., Xu, Y., et al., 2007. Mobilization and re-distribution of major and trace elements during extreme weathering of basalt in Hainan Island, South China. Geochim. Cosmochim. Acta 71 (13), 3223–3237.
Ma, J., Wei, G., Xu, Y., et al., 2010. Variations of Sr–Nd–Hf isotopic systematics in basalt during intensive weathering. Chem. Geol. 269 (3–4), 376–385.
Ma, Y., Liu, C., 2001. Sr isotope evolution during chemical weathering of granites: impact of relative weathering rates of minerals. Sci. China Ser. D 44 (8), 726–734 (in Chinese).
Ma, Y., Zhang, H., Xu, Z., et al., 2004. The Rb-Sr isotopic system in chemical weathering process: the mechanism and significance of the pseudo isochron diagram. Quat. Sci. 24 (1) (in Chinese).
Macleod, D.A., 1980. The origin of the Red Mediterranean soils in epirus, Greece. J. Soil Sci. 31 (1), 125–136.
Malpas, J., Duzgoren-Aydin, N.S., Aydin, A., 2001. Behaviour of chemical elements during weathering of pyroclastic rocks, Hong Kong. Environ. Int. 26 (5–6), 359–368.
Maynard, J., 1992. Chemistry of modern soils as a guide to interpreting Precambrian paleosols. J. Geol. 100 (3), 279–289.
Mee, A.C., Bestland, E.A., Spooner, N.A., 2004. Age and origin of Terra Rossa soils in the Coonawarra area of South Australia. Geomorphology 58 (1–4), 1–25.
Merino, E., Banerjee, A., 2008. Terra rossa genesis, implications for karst, and eolian dust: a geodynamic thread. J. Geol. 116 (1), 62–75.
Middelburg, J.J., van der Weijden, C.H., Woittiez, J.R.W., 1988. Chemical processes affecting the mobility of major, minor and trace elements during weathering of granitic rocks. Chem. Geol. 68 (3–4), 253–273.
Monroe, W., 1986. Examples of the replacement of limestone by clay. Miss. Geol. 7 (1), 1–6.
Moresi, M., Mongelli, G., 1988. The relation between the terra rossa and the carbonate-free residue of the underlying limestones and dolostones in Apulia, Italy. Clay Miner. 23, 439–446.
Négrel, P., Deschamps, P., 1996. Natural and anthropogenic budgets of a small watershed in the Massif Central (France): chemical and strontium isotopic characterization of water and sediments. Aquat. Geochem. 2 (1), 1–27.
Négrel, P., Guerrot, C., Millot, R., 2007. Chemical and strontium isotope characterization of rainwater in France: influence of sources and hydrogeochemical implications. Isot. Environ. Health Stud. 43 (3), 179–196.
Nesbitt, H., Young, G., 1989. Formation and diagenesis of weathering profiles. J. Geol. 97 (2), 129–147.
Nesbitt, H., Young, G., McLennan, S., et al., 1996. Effects of chemical weathering and sorting on the petrogenesis of siliciclastic sediments, with implications for provenance studies. J. Geol. 104 (5), 525–542.
Nesbitt, H., Markovics, G., Price, R.C., 1980. Chemical processes affecting alkalis and alkaline earths during continental weathering. Geochim. Cosmochim. Acta 44 (11), 1659–1666.
Nesbitt, H., Young, G., 1982. Early Proterozoic climates and plate motions inferred from major element chemistry of lutites. Nature 299 (5885), 715–717.
Nesbitt, H., Young, G., 1984. Prediction of some weathering trends of plutonic and volcanic rocks based on thermodynamic and kinetic considerations. Geochim. Cosmochim. Acta 48 (7), 1523–1534.
Olson, C.G., Ruhe, R.V., Mausbach, M.J., 1980. The Terra Rossa limestone contact phenomena in Karst, Southern Indiana. Soil Sci. Soc. Am. J. 44 (5), 1075–1079.
Pett-Ridge, J.C., Derry, L.A., Barrows, J.K., 2009. Ca/Sr and $^{87}Sr/^{86}Sr$ ratios as tracers of Ca and Sr cycling in the Rio Icacos watershed, Luquillo Mountains, Puerto Rico. Chem. Geol. 267 (1–2), 32–45.
Prasad, G., 1983. On the origin of red clays on Quaternary limestone along the East African coast. Z. Geomorphol. 48 (Suppl), 51–64.
Ruxton, B.P., Berry, L., 1957. Weathering of granite and associated erosional features in Hong Kong. Geol. Soc. Am. Bull. 68 (10), 1263.
Sequeira Braga, M.A., Paquet, H., Begonha, A., 2002. Weathering of granites in a temperate climate (NW Portugal): granitic saprolites and arenization. Catena 49 (1–2), 41–56.
Sposito, G., 2008. The Chemistry of Soils. Oxford University Press, New York, 329 pp.
Stephenson, L.W., 1939. Fossil Mollusks Preserved as Clay Replacements, near Pontotoc, Mississippi. J. Paleontol. 13 (1), 96–99.
Stewart, B.W., Capo, R.C., Chadwick, O.A., 2001. Effects of rainfall on weathering rate, base cation provenance, and Sr isotope composition of Hawaiian soils. Geochim. Cosmochim. Acta 65 (7), 1087–1099.
Sun, C., Wang, S., Liu, X., et al., 2002. Geochemical characteristics and formation mechanism of rock-soil interface in limestone weathering crust at Huaxi, Guizhou province. Acta Mineral. Sin. 22 (2), 126–132 (in Chinese with English abstract).
Syers, J.K., Jackson, M.L., Berkheiser, V.E., et al., 1969. Eolian sediment influence on pedogenesis during the quaternary. Soil Sci. 107 (6), 421–427.
Taylor, A.B., Velbel, M.A., 1991. Geochemical mass balances and weathering rates in forested watersheds of the southern Blue Ridge II. Effects of botanical uptake terms. Geoderma 51 (1–4), 29–50.
Taylor, A.S., Lasaga, A.C., 1999. The role of basalt weathering in the Sr isotope budget of the oceans. Chem. Geol. 161 (1–3), 199–214.
Vance, D., Teagle, D.A.H., Foster, G.L., 2009. Variable Quaternary chemical weathering fluxes and imbalances in marine geochemical budgets. Nature 458 (7237), 493–496.
Vilomet, J., Angeletti, B., Moustier, S., et al., 2001. Application of strontium isotopes for tracing landfill leachate plumes in groundwater. Environ. Sci. Technol. 35 (23), 4675–4679.
Wang, S., Ji, H., Ouyang, Z., et al., 1999. Preliminary study on weathering and pedogenesis of carbonate rock. Sci. China Ser. D 42 (6), 572–581 (in Chinese).
Wang, S., Sun, C., Feng, Z., et al., 2002. Mineralogical and geochemical characteristics of the limestone weathering profiles in Jishou, western Hunan province, China. Acta Mineral. Sin. 22 (1), 19–29 (in Chinese with English abstract).
Wang, X., Ji, H., Wang, s., 2007. A leaching experiment in dolomite weathering profile in centrial Guizhou and Geochemical characteristics. Geol. Rev. 53 (6), 830–838 (in Chinese with English abstract).
White, A.F., Brantley, S.L., 1995. Chemical weathering rates of silicate minerals: an overview. Rev. Mineral. 31, 1–22.

Wickman, T., Jacks, G., 1993. Base cation nutrition for pine stands on lithic soils near Stockholm, Sweden. Appl. Geochem. 8, 199–202.
Worden, J.M., Compston, W., 1973. A Rb-Sr isotopic study of weathering in the Mertondale granite, Western Australia. Geochim. Cosmochim. Acta 37 (12), 2567–2576.
Yaalon, D.H., Ganor, E., 1973. The influence of dust on soils during the quaternary. Soil Sci. 116 (3), 146–155.
Young, G.M., Nesbitt, H.W., 1998. Processes controlling the distribution of Ti and Al in weathering profiles, siliciclastic sediments and sedimentary rocks. J. Sediment. Res. 68 (3), 448.
Zhu, L., Li, J., 2004. Weathering and Pedogenesis of Carbonate Rocks and Their Environmental Effects. Geology Press, Beijing, 113 pp (in Chinese).